

---

**Ulm University**

**Institute of Orthopaedic Research and Biomechanics**

**Director: Prof. Dr. Anita Ignatius**

The role of complement component C6 and the  
MAC-regulator CD59a in skeletal homeostasis

Dissertation

for the Doctoral Degree in Medicine

(Dr. med)

from the Medical Faculty, Ulm University

**Zhaozhou Ren**

born in Shenyang, Liaoning, China

2018

---

Dean: Prof. Dr. Thomas Wirth

First Reviewer: Prof. Dr. Anita Ignatius

Second Reviewer: Prof. Dr. Rolf Brenner

Day doctorate awarded: 10.05.2019

## Contents

### List of contents

### List of abbreviations

<b>1</b>	<b>Introduction</b>	1
1.1	Bone remodeling	1
1.1.1	Bone formation and osteoblasts	1
1.1.2	Osteocytes	3
1.1.3	Bone resorption and osteoclasts	4
1.2	Bone loss	6
1.3	Complement cascade	7
1.4	Interaction of complement and bone cells	10
1.4.1	Complement and osteoblasts	10
1.4.2	Complement and osteoclasts	11
1.5	Complement and skeletal diseases	13
1.5.1	Complement and rheumatoid arthritis	13
1.5.2	Complement is involved in osteoarthritis or periodontitis	15
1.6	Aim of the study	17
<b>2</b>	<b>Methods and materials</b>	18
2.1	Animal model and husbandry	18
2.2	Biomechanical testing	19
2.3	Micro-computed tomography ( $\mu$ CT) analysis	19
2.4	Histomorphometric analysis	22
2.5	Statistical analysis	22
<b>3</b>	<b>Results</b>	23
3.1	Influence of C6 deficiency and CD59a knock-out on trabecular bone	23
3.1.1	Influence of C6 deficiency on trabecular bone	23

---

Global deficiency of C6 reduces trabecular bone mass in distal femur from 17-week-old mice .....	23
Global deficiency of C6 reduces spinal trabecular bone mass .....	25
3.1.2 Global deficiency of C6 increases osteoclast surface of distal femur and spine .....	27
3.1.3 Global deletion of C6 has no effect on osteoblast number and surface .....	29
3.1.4 Influence of CD59a deficiency on trabecular bone .....	31
Global deletion of CD59a reduces trabecular bone mass of distal femur in 17-week-old mice .....	31
Global deletion of CD59a has no effect on trabecular bone of spine .....	33
3.1.5 Global deletion of CD59a in mice increases the number of osteoclasts in femur but not in spine .....	35
3.1.6 Global deficiency of CD59a has no effect on osteoblast number and surface .....	37
3.2 Influence of C6-deficiency and CD59a knock-out on cortical bone .....	39
3.2.1 Global deletion of C6 decreases mineral density of cortex in femur from 34-week-old mice, with no alterations in cortical thickness .....	39
3.2.2 Global deficiency of C6 has no effect on bending stiffness .....	40
3.2.3 Global deletion of CD59a reduces mineral density of cortex in femur, with no alterations in Ct.Th .....	40
3.2.4 Increased bending stiffness in CD59a-deficient mice is due to the alterations of bone geometry at 34 weeks of age .....	41
<b>4 Discussion .....</b>	<b>43</b>
4.1 The role of CD59a and C6 in bone homeostasis .....	43
4.2 Age-related changes and the peak mass in skeletal architecture .....	46
<b>5 Summary .....</b>	<b>49</b>
<b>6 References .....</b>	<b>51</b>
<b>7 List of figures and table .....</b>	<b>63</b>
<b>8 Acknowledgements .....</b>	<b>65</b>
<b>9 Curriculum Vitae .....</b>	<b>67</b>

## List of abbreviations

### (Abbreviation) Definition:

- (ADAMTSs) disintegrin-like and metallopeptidase with thrombospondin type 1 motif
- (AIA) antibody-induced arthritis
- (ALP) alkaline phosphatase
- (BFR/BS) the ratio of bone formation rate and bone surface
- (BM) bone marrow
- (BMC) bone mineral content
- (BMD) bone mineral density
- (BMPs) bone morphogenetic proteins
- (BMSCs) bone marrow stromal cells
- (BV/TV) trabecular bone volume fraction, the bone volume/tissue volume
- (C1、C2、C3~C9) complement component 1, 2, 3 ~complement component 9
- (C1qr2s2) C1 complex
- (C3G) C3 glomerulopathy
- (CAIA) collagen and antibody-induced arthritis
- (C5aR1) C5a receptor 1, or termed CD88
- (C5aR2) C5a receptor 2, or termed C5L2
- (C4b2b) convertase of complement component 3
- (C3bBb) convertase of complement component 3
- (C4b2b3b or C3bBb3b) C5 convertases
- (CCL2, or termed MCP-1) chemokine (C-C motif) ligand 2, or monocyte chemotactic protein 1
- (CCL5) chemokine (C-C motif) ligand 5
- (CCL22) C-C motif chemokine ligand 22, or termed CCR4
- (CIA) collagen-induced arthritis
- (COX-2) cyclo-oxygenase 2
- (CRIg) complement receptor of the immunoglobulin superfamily

- (CSF1) colony-stimulating factor 1
- (Ct.Th) cortical thickness
- (CXCL1) chemokine (C-X-C motif) ligand 1
- (DMP-1) dentine matrix protein-1
- (DXA) dual energy X-ray absorptiometry
- (EI) flexural rigidity, or termed bending stiffness
- (FB) factor B
- (FD) factor D
- (FSH) follicle-stimulating hormone
- (GCF) gingival crevicular fluid
- (HA) hydroxyapatite
- (hMSCs) human mesenchymal stem cells
- (HSCs) haematopoietic stem cells
- (IGF-1) insulin-like growth factor-1
- (IL-1 $\beta$ ) interleukin-1 $\beta$
- (IL-6) interleukin-6
- (IL-8) interleukin-8
- (JAK-STAT) janus kinase-signal transducer and activator of transcription
- (Ma.Ar) marrow area
- (MAC) membrane attack complex
- (MAPK) mitogen-activated protein kinases
- (MAR) mineral apposition rate
- (MASPs) MB lectin-associated serine proteases
- (MB) mannose-binding
- (M-CSF) macrophage colony-stimulating factor
- (Micro-CT, or  $\mu$ CT) micro-computed tomography
- (MMP1) matrix metalloprotease 1
- (MMP 3) matrix metalloprotease 3
- (MMP 9) matrix metalloprotease 9

- (MMP13) matrix metalloprotease 13
- (MOI) moment of inertia in X axis
- (MPs) mesenchymal progenitors
- (MSCs) mesenchymal stem cells
- (NF- $\kappa$ B) nuclear factor kappa-light-chain-enhancer of activated B cells
- (N.Ob/B.Pm) the number of osteoblasts per bone perimeter
- (N.Oc/B.Pm) the number of osteoclasts per bone perimeter
- (OA) osteoarthritis
- (Ob.S/BS) the osteoblast surface per bone surface
- (Oc.S/BS) the osteoclast surface per bone surface
- (OPG) osteoprotegerin
- (OPGL) osteoprotegerin ligand
- (OS/BS ratio) osteoid surface per bone surface
- (PBMNC) peripheral blood mononuclear cells
- (pMOI) polar moment of inertia
- (PRM) pattern recognition molecule
- (PTGS2) prostaglandin-endoperoxide synthase 2
- (QCT) quantitative computed tomography
- (RA) Rheumatoid arthritis
- (RANK) receptor activator of nuclear factor kappa-B
- (RANKL) receptor activator of nuclear factor kappa-B ligand
- (ROI) region of interest
- (RUNX2) runt-related transcription factor 2
- (sCR1) soluble complement receptor 1, or termed CD35
- (Tb) trabecular
- (Tb.N) trabecular number
- (Tb.Sp) trabecular separation
- (Tb.Th) trabecular thickness
- (TGF- $\beta$ ) transforming growth factor beta
- (TMD) tissue mineral density

(TNF- $\alpha$ ) tumor necrosis factor alpha

(TNFSF11)TNF ligand superfamily member 11

(TRANCE)TNF-related activation-induced cytokine

(TRAP) tartrate-resistant acid phosphatase

(Tt.Ar) total cross-sectional area inside the periosteal envelope

(Wnts) wingless-ints

(WT) wild type



## **1 Introduction**

### **1.1 Bone remodeling**

The skeleton is constituted of mineral (50 to 70%), organic matrix (20 to 40%), water (5 to 10%), and lipids (<3%). The mineral composition of skeleton is mostly hydroxyapatite  $[\text{Ca}_{10}(\text{PO}_4)_6(\text{OH})_2]$ , few carbonate, magnesium, and acid phosphate. Mineral composition supports bone mechanical stiffness and load-bearing strength, while the organic matrix supplies skeletal elasticity and flexibility [1]. Bone remodeling is a process by which skeleton is self-renewed to preserve bone strength and mineral homeostasis. Osteoclasts carry out resorption of old bone, whereas osteoblasts produce new organic matrix and also regulate mineralization of matrix through the accumulation of calcium phosphate in the form of hydroxyapatite [1, 2].

#### **1.1.1 Bone formation and osteoblasts**

Mesenchymal stem cells (MSCs) are multipotent stromal cells that can differentiate into several types of cells, including osteoblasts, chondrocytes, myocytes, fibroblasts, and adipocytes (Fig. 1) [1, 3]. The initial step of osteoblastogenesis involves the development of MSCs to osteochondroprogenitor cells, which subsequently have the ability to differentiate into osteoblasts or chondrocytes. Several hormones, cytokines, and signaling molecules are involved in the process of osteoblastogenesis, including PTH, prostaglandin, interleukin (IL)-11, insulin-like growth factor-1 (IGF-1) and TGF- $\beta$  receptors [2, 3]. Wntless-ints (Wnts) and bone morphogenetic proteins (BMPs) are mainly involved in the early differentiation [2, 3]. Additionally, runt-related transcription factor 2 (RUNX2) directs early differentiation of osteoblasts and is expressed in both preosteoblasts and osteoblasts [3].

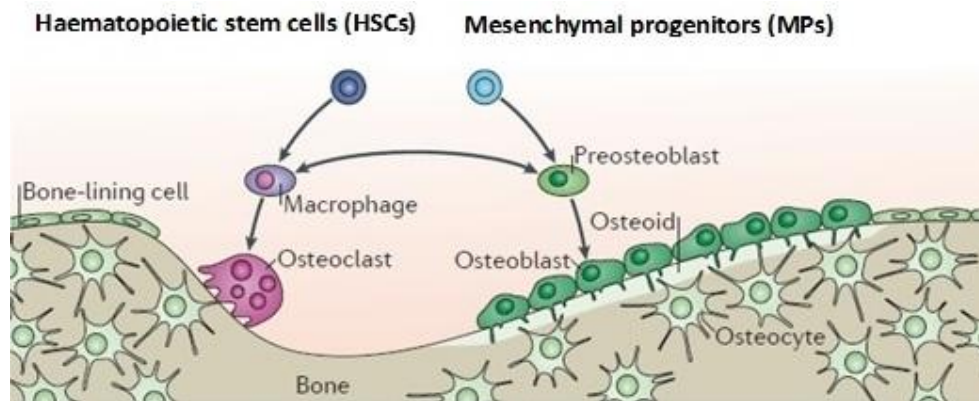


**Figure 1: Bone homeostasis is controlled by the interplay of osteoblasts, osteoclasts and osteocytes (Ref. 3, page 28, figure 1).** Cells of the hematopoietic lineage differentiate to osteoclasts, which resorb bone. Osteoblasts originating from mesenchymal progenitors deposit new bone to fill up the resorption cavities. “Republished with permission of [Springer Nature], from [Ref. 3]; permission conveyed through Copyright Clearance Center, Inc.”

In the early phase of bone formation, osteoid, the non-mineralized bone matrix, is deposited by osteoblasts and is subsequently mineralized by releasing and extruding membrane-bound matrix vesicles that concentrate calcium and phosphate (Fig. 1) [2, 3]. About 90% of osteoid is type I collagen, however, osteoblasts also secrete non-collagenous extracellular matrix proteins, including alkaline phosphatase (ALP), osteocalcin (Gla proteins), and osteonectin, that regulate the deposition of bone mineral, influence the activity of bone cells and cell-attachment, and support the turnover of bone matrix (Table 1) [1-5]. ALP first extrudes calcium-nucleated vesicles and enzymatically cleaves pyrophosphate to form the incomplete hydroxyapatite crystals [2-5]. Phosphoprotein kinases and phosphatases control the growth of the crystals and increase calcium ions by the phosphorylation of the key nucleating phosphoproteins, bone sialoprotein and dentine matrix protein-1 (DMP-1) [2-5].

**Table 1: Matrix proteins and their skeletal functions (Ref. 1, page S136; Ref. 2, page 793).**

<b>Protein</b>	<b>Function</b>
Versican	Determinant of space
Biglycan	Collagen fibril formation and correlation with peak bone mass
Bone sialoprotein	Activates mineralization
Osteonectin	Regulates collagen fibril and mineralization
Osteopontin	suppresses mineralization
Osteocalcin	Regulates osteoclasts and inhibits mineralization
Matrix Gla protein	Inhibits mineralization
RGD-containing glycoproteins (thrombospondins, fibronectin, vitronectin, fibrillin 1 and 2)	Cell attachment

“Republished with permission of [AMERICAN SOCIETY OF NEPHROLOGY] and [Springer Nature] respectively, from [Ref. 1] and [Ref. 2] respectively; permission conveyed through Copyright Clearance Center, Inc.”

### 1.1.2 Osteocytes

After the completion of bone formation, mature osteoblasts have three potential fates. They can become quiescent lining cells on the bone surface, undergo apoptosis, or differentiate terminally to osteocytes that are embedded in lacunae within the mineralized matrix of bone (Fig. 2) [6-10].

Osteocytes are the master signal sensor, integrator, and transducer of the skeleton, and make up more than 95% of bone cells in the mature bone tissue. Osteocytes send their dendritic processes to form the lacunocanalicular network (Fig. 2), which connects bone cells to the bone surface and to the adjacent vasculature [9, 10], providing oxygen and nutrients to maintain the viability of the cell in this enclosed environment. Through fluid flow in the osteocyte-lacunocanalicular network, osteocytes sense and respond to changes arising from stress, strain or pressure [9-11].

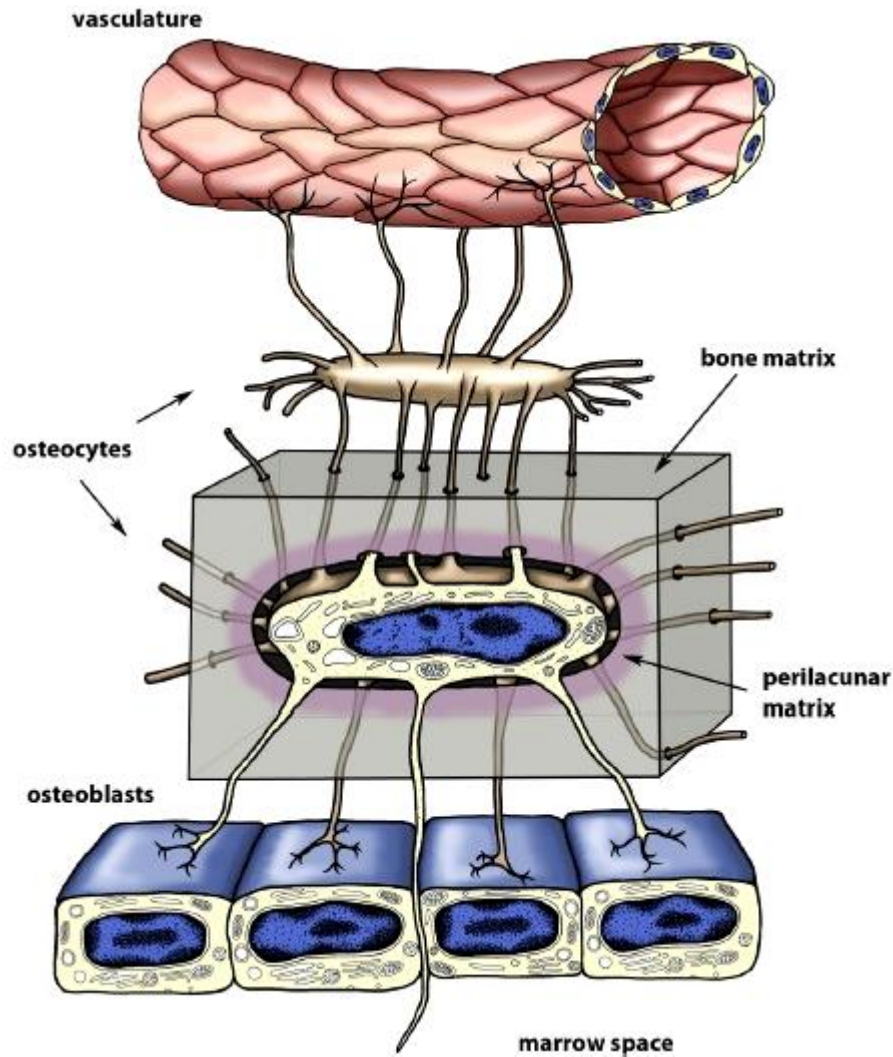


**Figure 2: Osteocytes are terminally differentiated osteoblasts embedded into the bone matrix (Ref. 10, page 659, figure 1).** Via their dendritic processes, osteocytes are connected to osteoblasts lining the bone surface, other osteocytes, and the vasculature. “[Dallas SL, Prideaux M, Bonewald LF. The osteocyte: an endocrine cell ... and more. *Endocr Rev.* 2013;34:658-690], by permission of Oxford University Press or Endocrine Society, and by permission conveyed through Copyright Clearance Center, Inc.”

### 1.1.3 Bone resorption and osteoclasts

Precursors of osteoclasts are derived from the monocyte/macrophage lineage, which originates from haematopoietic stem cells (HSCs) in the bone marrow [12, 13]. The receptor activator of nuclear factor kappa-B ligand (RANKL), also known as TNF ligand superfamily member 11 (TNFSF11) or TNF-related activation-induced cytokine (TRANCE) or OPGL from osteoblast lineage cells, was first mentioned as a T cell-derived cytokine enhancing T-cell growth and dendritic cell function [14].

Besides this function in the immune system, RANKL is also the critical downstream effector cytokine for osteoclast formation and bone resorption [15-18]. Another important mediator in osteoclastogenesis is macrophage colony-stimulating factor (M-CSF), a cytokine secreted by cells of the monocyte-macrophage-osteoclast lineage that influences HSCs to differentiate into macrophages, monocytes or osteoclasts [15-18].

In the presence of M-CSF, RANKL is considered to bind solely to its receptor RANK (also known as TNFRSF11A) on osteoclast precursors and promotes their differentiation into pre-osteoclasts, which terminally differentiate into mature osteoclasts [15-18]. RANKL and M-CSF are essential for osteoclastogenesis, as mice lacking either protein fail to produce osteoclasts and eventually develop osteopetrosis [19, 20]. Osteoprotegerin (OPG), also known as TNFSF11B, is a physiological decoy receptor of RANKL and an effective inhibitor of osteoclast differentiation. The RANKL to OPG ratio is anticipated to be a pivotal determinant of osteoclast differentiation and activity (Fig. 3) [21, 22]. In humans, autosomal-recessive inactivating mutations of the TNFSF11B gene (OPG deficiency) cause juvenile Paget's disease, which is characterized by high-turnover bone loss, dental lysis, focal appendicular bone lesions and deafness. As expected, anti-resorptive bisphosphonates are helpful and effective for these patients [23].

Previously, osteoblasts and/or bone marrow stromal cells were thought to be the main source for RANKL and OPG. However, recent studies showed that osteocytes are the major source of RANKL in bone remodeling [24, 25]. Moreover, osteocyte RANKL is responsible for unloading-induced bone loss [24, 25].

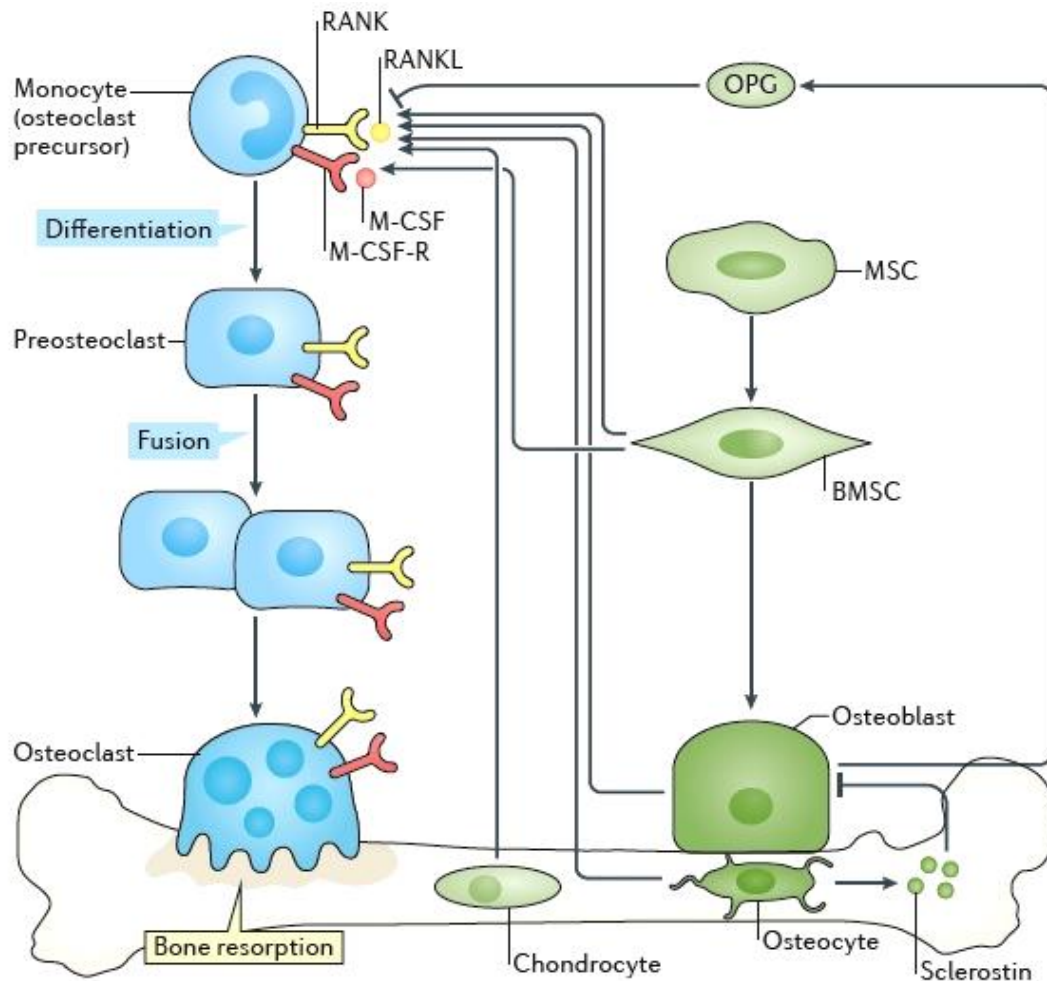


**Figure 3: Role of the RANK-RANKL-OPG system in osteoclast formation (Ref. 106, page 520, figure 1).** RANKL and OPG are the key downstream effectors of osteoclast-mediated resorption of bone. Macrophage colony-stimulating factor 1 (M-CSF) and RANKL promote the differentiation of monocytes into pre-osteoclasts, that fuse to mature osteoclasts. OPG inhibits osteoclast formation by acting as decoy receptor for RANKL. “Republished with permission of [Springer Nature], from [Ref. 106]; permission conveyed through Copyright Clearance Center, Inc.”

## 1.2 Bone Loss

Bone loss emerges when there is an imbalance between osteoclastic bone resorption and osteoblastic bone formation temporally or spatially [2]. High-turnover bone loss is characterized by an absolute increase in bone resorption with a relative but insufficient increase in bone formation. This occurs as a result of hypogonadism, i.e. estrogen deficiency in women and testosterone deficiency, thyrotoxicosis, hyperparathyroidism, the diseases of cytokine excess, skeletal metastases, Paget’s bone disease, rheumatoid arthritis and periodontitis [2].

Estrogen, is not only a potent anti-inflammatory hormone, but also plays a fundamental role in skeletal growth and bone homeostasis in humans, as estrogen is considered as a potent factor of bone protection [26]. Following menopause, estrogen deficiency in women causes an increase in bone resorption by increasing osteoclastogenesis, decreasing the apoptosis of osteoclasts and increasing the activity of osteoclasts, and consequently leads to postmenopausal osteoporosis [27]. Fast and abundant bone loss initiates 3 years before the last menstrual period, whereas serum estrogen is relatively normal. Elevated follicle-stimulating hormone (FSH) causes the sharp early hyper-resorption that accompanies hypogonadism. An increase in the pituitary hormone, FSH, might be an early event instigating an increase in bone resorption [28]. There are also tight correlations between elevated serum FSH and bone loss during the early post-menopause in amenorrheic women [29, 30]. In contrast, low-turnover bone loss is characterized by the decrease in both bone formation and bone resorption. This appears as a result of aging, disuse and excess glucocorticoids [2].

Chronic inflammation and NF- $\kappa$ B pathway contribute to osteoporosis and aging-related bone loss [31, 32-33]. By generating transgenic mice that express Wnt4 especially in osteoblasts, Yu et al. have reported that Wnt4 is able to protect against natural age-related bone loss and estrogen deficiency-induced bone loss by targeting NF- $\kappa$ B signaling, concurrent with decreased levels of TNF, COX-2, and MMP9 [31]. Additionally, early-life IGF-1 deficiency can inhibit age-related loss of vertebral bone volume and bone density in female mice, concurrent with an elevated ratio of OPG/RANKL levels and increased osteoblast surface [34].

### **1.3 The complement cascade**

The complement system belongs to the innate immune system, and it usually leads to the body's counterattack against bacteria by controlling microbial threats and eliminating cellular debris. In contrast to the adaptive immune system, complement components eliminate pathogens swiftly and are always ready for initiation and amplification. Although traditionally complement system is primarily viewed as a

host defense system against microbial invaders, it is now understood to contribute to various immune, inflammatory, neurodegenerative, ischemic, osteoarthritis, and age-related diseases [35-38].

The complement system consists of three distinct pathways, including classical pathway, mannose-binding (MB) lectin pathway and alternative pathway, which eventually converge at the generation of the C3 and C5 convertases (Fig. 4) [35-38]. The classical pathway is initiated by IgG or IgM clusters and is thought to be antibody-dependent. When recognizing distinct structures on microbial and apoptotic cells, the pattern recognition molecule (PRM) C1q binds the proteases C1r and C1s to form C1 complex (C1qr2s2) (Fig. 4). C1s subsequently cleaves C4 into C4a and C4b, leading to exposure of hidden thioester and covalent deposition of C4b on activation surfaces. Through thioester moiety, activation of C4 produces the opsonin C4b. Additionally, C1s also mediates the generation of the C3 convertase (C4b2b) [35-38].

In the MB-lectin pathway, C1q, C1r, C1s, MB lectin, ficolins, and collectin-11 form MB lectin-associated serine proteases (MASPs), and they predominantly recognize carbohydrate patterns on microbial and apoptotic cells. Similar to the classical pathway, MASPs cleave C4 and C2, and the activation of C4 subsequently generates C4b (Fig. 4). Conversely, the cleavage fragment of C2 binds to C4b to generate the C3 convertase (C4b2b), which is able to cleave C3 into activated fragments, the anaphylatoxin C3a and the versatile opsonin C3b [35-38].

In the presence of factor B (FB) and factor D (FD), surface-deposited C3b can form the major alternative pathway C3 convertase (C3bBb), which subsequently activates additional C3 to form C3b and generate more C3 convertases, supplying an efficient loop to markedly amplify the response and the subsequent effector functions (Fig. 4). The alternative pathway might contribute most to complement activation and response [39].

The alternative pathway amplifies the density of C3b opsonin on the target surface, subsequently resulting in the formation of C5 convertases (C4b2b3b or C3bBb3b), which are able to cleave C5 into the anaphylatoxin C5a and into C5b. Consequently, C5b associates with C6 and C7, leading to a stable complex, which inserts into cell



membranes and eventually forms membrane attack complex (MAC, C5b–9<sub>n</sub>) through binding to C8 and several units of C9 [35-37, 40].

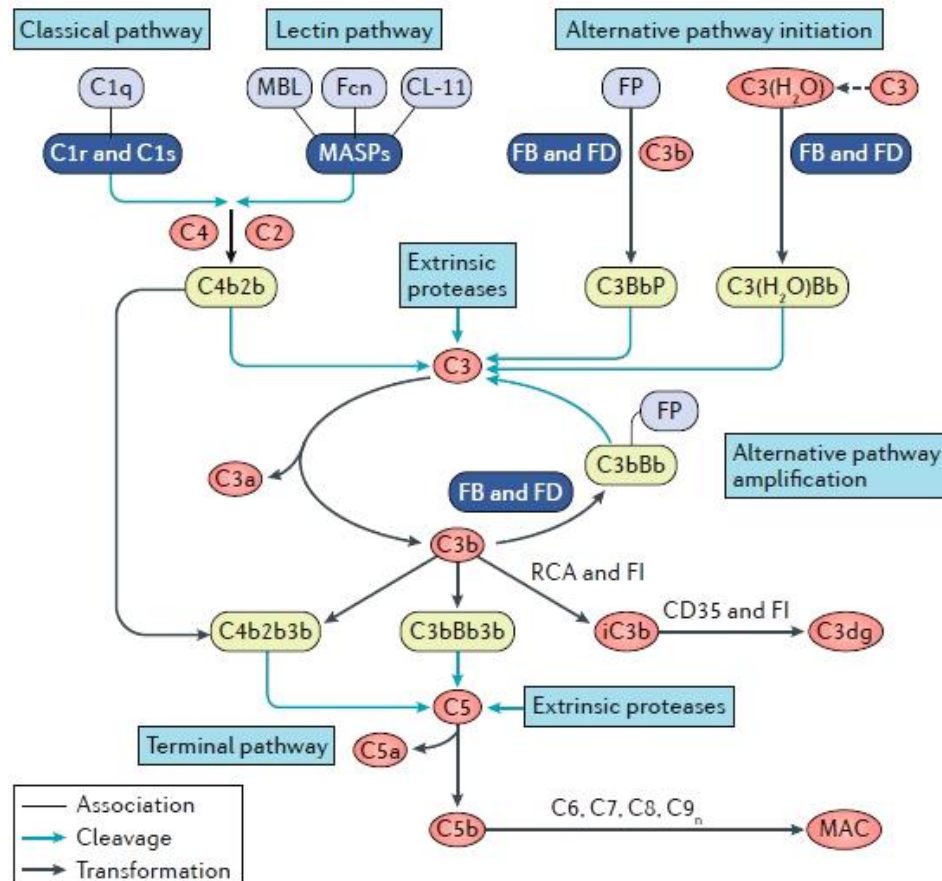


**Figure 4: Overview of the complement cascade with its different activation pathways (Ref 37, page 385, Box 1).** All pathways converge at the level of complement component C5. “Republished with permission of [Springer Nature], from [Ref. 37]; permission conveyed through Copyright Clearance Center, Inc.”

The MAC, as well as the anaphylatoxins C5a and C3a, are the major effector components of complement. The MAC binds to cell membranes and forms a transmembrane pore that leads to damage and lysis of the target cell [35-37, 41]. Not all cells are susceptible to MAC-induced cell lysis, it mainly appears in aged erythrocytes and certain Gram-negative bacteria [37]. Importantly, cell lysis is not the only effector function of MAC. MAC also can promote inflammation by activating pro-inflammatory cell signalling, when it binds to the cell surface at sublytic levels [41, 42]. Consequently, pro-inflammatory signaling and phagocytosis are essential for

complement-mediated defense against foreign invaders [41, 42]. Of note, the membrane-bound regulator CD59 prevents the formation of both sublytic and lytic MAC by binding to active forms of C8 and C9 [41].

The anaphylatoxin C5a is a powerful chemoattractant that recruits neutrophils, monocytes, and macrophages towards the sites of activation by binding to C5a receptor 1 (C5aR1 or CD88). The role of a second C5a receptor (C5aR2 or C5L2) is not completely clarified. Compared to the potent pro-inflammatory effect of C5a, the activity of C3a seems to be more versatile and context-specific as a particular inflammatory modulator [37]. C3a is unable to attract neutrophils, but might even neutralize the neutrophil-attractant effects of C5a by promoting direct anti-microbial activity [43, 44].

### **1.4 Interaction of complement and bone cells**

#### **1.4.1 Complement and osteoblasts**

It was shown previously, that human MSCs (hMSCs) and osteoblasts express C3, C5, C3aR, C5aR, the membrane-bound regulatory proteins CD46, CD55, and CD59 [45]. Furthermore, osteoblasts were also able to activate complement by cleaving C5 to its active form C5a. Stimulation with C3a or C5a did not affect osteogenic differentiation. Co-stimulation with IL-1 $\beta$ /C3a or IL-1 $\beta$ /C5a in human osteoblasts significantly increased the concentration of IL-6 and IL-8, as well as the mRNA expression of RANKL and OPG. This indicates that complement may regulate the inflammatory response in osteoblasts and supplies a pro-inflammatory environment, which is involved in the interaction between osteoblasts and osteoclasts [45]. However, C3a or C5a alone was not able to trigger the release of IL-6 and IL-8 from osteoblasts, but they may promote the inflammatory response in osteoblasts and increase osteoclast formation, particularly in a pro-inflammatory environment [45].

Regarding complement receptor, C5aR mRNA was nearly undetectable in undifferentiated hMSC, but its expression was significantly triggered and increased

during differentiation of hMSC toward the osteogenic phenotype *in vitro* [46]. Furthermore, during the process of osteogenic differentiation *in vitro*, C5a induced more migrated cells under indirect migratory response of human primary osteoblasts as a concentration-dependent feature (from 10 ng/mL to 1000 ng/mL). In contrast, cell migration of undifferentiated hMSC was significantly induced only by the highest C5a concentration [46].

Complement proteins are also expressed in a specific spatial arrangement in the growth plate during bone development: C3 and Factor B located evenly in the resting and proliferation zones, while C5 and C9 located especially in the hypertrophic zones [47].

With regard to the effects of CD59a in osteoblast formation *ex vivo*, Bloom et al. showed there were no significant differences in the ALP staining and mineralisation between bone marrow (BM) osteoprogenitor cells from male WT and CD59a<sup>-/-</sup> mice, during the process of osteogenesis [48]. This indicates that CD59a does not affect osteoblast formation from BM osteoprogenitor cells *in vitro*. However, the authors found that the ratio of osteoid surface and bone surface *in vivo* was two-fold lower in male CD59a<sup>-/-</sup> mice at 8 weeks of age than in WT mice, while mineral apposition rate (MAR) and the ratio of bone formation rate and bone surface (BFR/BS) were both significantly increased in male CD59a<sup>-/-</sup> mice at 8 weeks of age [48]. Additionally, immunohistochemical staining for osteopontin *in vivo* showed an increase in femoral osteoblasts, osteoclasts, bone lining cells and megakaryocytes in femora of CD59a<sup>-/-</sup> male mice [48].

### 1.4.2 Complement and osteoclasts

Several studies have shown that complement components or regulators influence osteoclast formation or differentiation by direct and indirect effects [45-48, 49]. Tu et al. reported that BM cells from C3<sup>-/-</sup> mice displayed significantly reduced osteoclast differentiation by almost 50%, accompanied by less M-CSF and a decreased RANKL/OPG-ratio. Moreover, during osteoclast differentiation, murine BM cells locally produced C3, C5, factor B, and factor D through alternative pathway of

complement activation [49]. In addition, blocking C3a receptor (C3aR) by using C3aR antagonist in murine BM cell cultures significantly inhibited TRAP-positive osteoclast differentiation, whereas blocking C5a receptor (C5aR) by using C5aR antagonist did not significantly reduce the number of TRAP-positive cells. BM cells from C3aR<sup>-/-</sup> or C5aR<sup>-/-</sup> mice generated fewer number of TRAP-positive osteoclasts, following the same protocol of 1,25(OH)<sub>2</sub> vitamin D<sub>3</sub>-stimulated osteoclast differentiation. BM cells from double-knockout for C3aR<sup>-/-</sup> and C5aR<sup>-/-</sup> produced the least number of TRAP-positive osteoclasts. Similarly, human BM cells generated C5, factor B, and factor D during osteoclast differentiation. Furthermore, blocking C3aR or/and C5aR by using C3aR antagonist or/and C5aR antagonist in human BM cell cultures significantly inhibited osteoclast differentiation [49]. After the stimulation of C3aR or C5aR, monocytes or macrophages respectively produced IL-6, and IL-6 increased 1,25(OH)<sub>2</sub> vitamin D<sub>3</sub>-induced osteoclast differentiation from BM cells through IL-6R and gp130 [50, 51]. Of note, BM cells from C3<sup>-/-</sup> or C3aR<sup>-/-</sup> C3aR<sup>-/-</sup> mice generated decreased levels of IL-6 by 5 times during the process of osteoclast differentiation. Moreover, supplementation of IL-6 into C3<sup>-/-</sup> BM cells increased the number of TRAP-positive cells, whereas neutralization of IL-6 in WT or C3<sup>-/-</sup> BM cells with the stimulation of C3a/C5a efficiently abolished the effect of complement on osteoclast differentiation [49]. The authors deduced IL-6 could play an important role in complement regulated the process of osteoclast differentiation, and the production of IL-6 by BM cells is regulated by C3aR/C5aR during differentiation [49].

C3, C5, C3aR, C5aR as well as the membrane-bound regulatory proteins CD46, CD55, and CD59 were all expressed in human osteoclasts [45]. In the absence of RANKL and M-CSF, C3a or C5a significantly promoted osteoclastogenesis from peripheral blood mononuclear cells (PBMNC) directly. Furthermore, osteoclasts were able to activate complement by cleaving C5 to its active form C5a [45].

CD59 is the only complement modulator that inhibits the formation of MAC assembly and subsequently blocks the function of the lytic pore. During osteoclast differentiation *in vitro*, BM cells from male CD59a<sup>-/-</sup> mice generated significantly

more TRAP-positive cells than those from WT male mice with the supplementation of M-CSF and RANKL. Bone histomorphometry analysis *ex vivo* showed that osteoclast surface activity in the secondary spongiosa of CD59a<sup>-/-</sup> male mice was greater than that of WT mice at 8 and 20 week, and osteoclast number of CD59a<sup>-/-</sup> mice was also significantly increased at 20 weeks. However, there was no alteration in the number of TRAP-positive cells between age-matched female CD59a<sup>-/-</sup> and WT mice *in vitro* and *in vivo* study [48]. These gender-specific results emerged since complement system in male mice on the C57BL/6J background might be more active than female mice [52, 53]. Furthermore, the levels of CXCL1, a marker for osteoclast precursor cell recruitment, from male BMC osteoclastogenesis assays were significantly increased in CD59a<sup>-/-</sup> culture supernatants when treated with M-CSF compared to those of WT [48].

### 1.5 Complement and skeletal diseases

There is indirect evidence for the regulatory capacity of complement components or modulators in bone metabolism from human patients and from experimental models of rheumatoid arthritis, osteoarthritis, and periodontitis.

#### 1.5.1 Complement and rheumatoid arthritis

Rheumatoid arthritis (RA) is an autoimmune disease in which joint inflammation leads to cartilage degradation, bone destruction, and bone loss [54, 55]. About 56 % of female postmenopausal patients with RA have decreased bone mineral density (BMD) in at least one site (at the forearm, total hip, femoral neck, or lumbar spine) and consequently increased risk of fractures [56]. Complement components, such as C2, C3, C4 and C5, are significantly increased in cultures of synovial tissue obtained from patients with RA, compared to those from patients with degenerative or traumatic arthritis [57]. Therefore, it can be concluded that the local production of complement components is involved in the process and the inflammatory response in RA.

Components of the complement cascade are involved in the pathogenesis of collagen-induced arthritis (CIA). C3<sup>-/-</sup> mice exhibited almost complete resistance to

the induction of arthritis, while factor B-deficient mice were partly resistant to CIA [58]. Complement receptor of the immunoglobulin superfamily (CRIg) is a selective inhibitor of the alternative pathway of complement in human and mouse, as CRIg binds to the  $\beta$  chain of C3b and inhibits the C3 and C5 convertases [59]. By using mutants of the crystal structure of murine CRIg, inhibition of the alternative pathway not only reversed joint inflammation and clinical scores, accompanied with the reduced local IL-1 $\beta$  and IL-6 levels, but also reduced bone loss in experimental models of CIA and antibody-induced arthritis (AIA) [59]. The alternative pathway of complement is not only required for disease induction, but also for disease progression in RA [59, 60]. The soluble complement receptor 1 (CD35 or sCR1) is a potent inhibitor of the classical and alternative complement pathways as a deactivator of the C3 and C5 convertases. Injection of sCR1 prevented the progression of CIA and inhibited the development of joint inflammation in both rats [61] and mice [62]. Treatment with APT070, a membrane-targeting complement regulatory protein derived from human complement receptor 1, in animals led to significantly milder clinical and histologic disease in arthritis as a dose-dependent therapeutic effect, compared with vehicle controls or animals treated with APT898, an non-membrane-targeting control regulator [63]. For C5 component, systemic administration of anti-C5 monoclonal antibodies prevented the onset of collagen-induced arthritis (CIA) and ameliorated established disease in animal models by blocking the production of the major chemotactic and proinflammatory factors C5a and MAC C5b-9 [64]. C5-deficient mice were highly resistant to the induction of CIA despite equivalent intra-articular deposition of IgG and C3 on the cartilage surfaces [65].

In CD59a<sup>-/-</sup> mice, measurement of joint swelling and histological indicators of joint damage were significantly enhanced compared to WT controls in an experimental model of AIA [66]. The deposition of MAC in the arthritic joints from CD59a<sup>-/-</sup> mice was also increased [66]. The administration of sCD59-APT542, a novel membrane-targeted rat CD59 derivative, markedly ameliorated disease severity, leading to a reduction of knee swelling and joint damage in CD59a<sup>-/-</sup> mice [66]. In an

experimental model of CAIA, clinical scores and histopathologic injury of arthritis in C3aR<sup>-/-</sup>, C5aR<sup>-/-</sup>, and C6<sup>-/-</sup> mice were all reduced in comparison to WT mice [67]. The deposition of IgG and C3, and the percentage of synovial neutrophils were also decreased in all three genotypes compared to WT mice. Notably, the percentage of synovial macrophages was only decreased in C3aR<sup>-/-</sup> and C5aR<sup>-/-</sup>, but not in C6<sup>-/-</sup> mice. mRNA expression of TNF- $\alpha$  in synovium was decreased in C5aR<sup>-/-</sup> mice, whereas synovial mRNA IL-1 $\beta$  was reduced in both C5aR<sup>-/-</sup> and C6<sup>-/-</sup> mice. However, there was no alteration in either cytokine in C3aR<sup>-/-</sup> mice [67].

### 1.5.2 Complement is involved in osteoarthritis and periodontitis

Osteoarthritis (OA) has long been considered as a degenerative breakdown of articular cartilage resulting from ‘wear and tear’, but recent evidence indicates that inflammation has a pivotal role in its pathogenesis. The inflammation in OA is different from that in RA and other autoimmune diseases, where it is chronic and comparatively low-grade [38, 68].

Recent studies in human and mouse suggest that the complement system plays a central role in the pathogenesis of OA [38, 68]. Regarding the effector components, the C3a and C5a anaphylatoxins induce inflammation by chemoattracting pro-inflammatory leukocytes, while the MAC binds to cell membranes and forms a transmembrane pore that leads to lysis and damage of the target cell [69, 70]. The MAC also can promote inflammation by activating pro-inflammatory cell signalling, such as mitogen-activated protein kinases (MAPK), the Janus kinase-signal transducer and activator of transcription (JAK-STAT) pathway, and NF- $\kappa$ B, when it binds to the cell surface as sublytic MAC [41, 42]. Early studies have revealed that complement components and immunoglobulin deposit in articular cartilage [71] and synovium [72] of patients with OA. Recent report has shown that the expression and activation of complement are significantly higher in synovial joints of patients with OA than healthy individuals, through proteomic and transcriptomic analysis of synovial fluids and membranes [38]. Moreover, by using mice genetically deficient in complement components or the MAC regulatory protein, Wang et al. revealed that C5-deficient or

C6-deficient mice developed attenuated experimental OA, whereas deficiency in CD59a aggravated the process of OA [38]. However, many of the MAC-surrounded chondrocytes in osteoarthritic cartilage seemed to be morphologically normal [38]. The authors isolated chondrocytes from cartilage of OA patients, and incubated chondrocytes coated with or without sublytic MAC *in vitro*. They found that sublytic MAC not only increased the production of cartilage-degrading enzymes in cultured chondrocytes, including matrix metalloprotease (MMP) 1, MMP3, MMP13, and disintegrin-like and metallopeptidase with thrombospondin type 1 motif (ADAMTSs), cyclooxygenase 2 (COX-2), and prostaglandin-endoperoxide synthase 2 (PTGS2) [73-76], but also enhanced the expression of pro-inflammatory cytokines and mediators, such as C-C motif chemokine ligand (CCL) 2, CCL5, or colony-stimulating factor 1 (CSF1) [77]. Additionally, sublytic MAC also amplified pathogenic complement signalling in OA by inducing the expression of other complement effectors, such as C3 and C5. Furthermore, chondrocytes from the joints of C5-deficient mice expressed lower concentrations of inflammatory and degradative mediators than those from the joints of C5-sufficient mice, with decreased mRNA levels of the pro-inflammatory transcription factors Jun and Fos [78, 79].

Besides RA and OA, periodontitis is an oral and skeletal disease characterized by the inflammatory destruction of the tooth-supporting tissues, the periodontium, including alveolar bone and gingiva [80]. Periodontitis is associated with increased risk of some systemic conditions, such as RA and atherosclerosis [81, 82]. Complement is involved in the pathogenesis of periodontal dysbiosis and inflammatory bone loss [83]. Effective anti-periodontitis therapy not only attenuated periodontal inflammation and destruction, but also reduced activation of C3 in the gingival crevicular fluid (GCF) [84]. Moreover, the progression of gingival inflammation in human was correlated with increased C3 cleavage in the GCF [85].

Taken together, the complement system is a potent trigger and amplifier of local or systemic inflammation that causes bone atrophy and aberrant bone apposition.

### **1.6 Aim of the study**

The complement system has been recognized as a regulator of bone homeostasis



and it was also shown to contribute to the pathogenesis of musculoskeletal conditions such as rheumatoid arthritis and osteoarthritis. Previously, the focus of research was mostly on the complement components C3 and C5, their split products and respective receptors. The role of the terminal complement cascade downstream of C5 on bone homeostasis was investigated to a lesser extent. Therefore, the present study explored the role of the most terminal complement component, the membrane attack complex (MAC) as well as the role of the MAC-regulatory component CD59a in bone homeostasis.

In particular, the phenotype of trabecular and cortical bone was analyzed in mice lacking the complement component C6, therefore being unable to assemble the MAC, and in mice lacking the MAC-regulator CD59a.

## 2. Methods and Materials

### 2.1 Animal model and husbandry

All animal experiments were performed in compliance with the international and national recommendations for the care and use of laboratory animals, and were approved by the local ethics committee (o.135, Tierforschungszentrum Ulm University).

To study the influence of the MAC on bone homeostasis, the following models were used:

#### C6-deficient mice (C6-KO)

These mice were derived from mice naturally lacking complement component C6. The C6-deficiency was transferred to C57BL/6 background. The mice were provided by Prof. John D. Lambris from the University of Pennsylvania and bred at the Tierforschungszentrum of Ulm University.

#### CD59a-knockout mice (CD59a-KO)

The CD59a-KO mice were produced by targeted deletion of exon 2 of the gene for CD59a in embryonic stem cells [86]. The mice were provided by Wen-Chao Song from the University of Pennsylvania and bred at the Tierforschungszentrum of Ulm University.

C57BL/6J mice served as controls for C6-KO and CD59a-KO, and were purchased from Charles River (Sulzfeld, Germany).

The mice were housed in groups of up to 5 mice per MacrolonTypeII-cage at a 14 h light and 10 h dark rhythm. Food and water were accessible *ad libitum*. The mice were sacrificed by CO<sub>2</sub> asphyxiation.

The following groups and number of each group were analyzed:

**Table 2: C6-deficient (C6-KO) mice and CD59a-knockout (CD59a-KO) mice were used for this study of skeletal phenotyping. Age- and sex-matched C57BL/6 mice were used as wild-type (WT) controls.**

	genotype	C6-KO	CD59-KO	C57BL/6
age				
17 weeks		7	7	5
34 weeks		8	5	8

## 2.2 Biomechanical testing

The bending stiffness (flexural rigidity) of the femur was assessed by a non-destructive three-point bending test using a material testing machine (Zwick, Ulm, Germany) as described previously [87-89]. Briefly, the proximal end of the femur was stabilized in an aluminum cylinder with SelfCem (HeraeusKulzer, Hanau, Germany). Subsequently, the cylinder was fixed on a hinge joint, serving as the proximal support for the bending test, while the femoral condyle was placed on the bending support as the other side. The loading cycle (maximum force 5 N) of each femur was evaluated to define the flexural rigidity (EI) from the slope (k) of the load-deflection curve [87-89]. The bending load F was applied on the mid-shaft and was continuously recorded each time. Flexural rigidity was calculated as  $EI = k(a^2b^2/3l)$ , with “l” as the distance between both supports being 20 mm, with “a” being the distance between the load vector and the proximal support, and with “b” being the distance between the load vector and distal support [87-89].

## 2.3 Micro-computed tomography (μCT) analysis

We obtained right femurs from mice, dissected them free of soft tissues, fixed them in 4% formalin and scanned them within 48h by using micro-CT (Skyscan 1172, Bruker, Belgium). Similarly, we obtained lumbar spines (L4 or L5) from mice, fixed

them in 4% formalin for 1 week, then dehydrated them in graded ethanol, immersed them in 80% ethanol for at least 2 weeks, further dissected them free of soft tissues, and scanned them by using micro-CT.

We used image reconstruction software (NRecon) and data analysis software (CTAnalyser) to calculate the parameters of the trabecular bone in the metaphysis of distal femur or vertebral body, and the cortical bone in the middle of femoral diaphysis [31, 87-88, 90-92]. We set the scanner at a voltage of 50 kV and 200  $\mu$ A for mice at a resolution of 8  $\mu$ m approximately. For calibration of bone mineral density (BMD), two phantoms of hydroxyapatite (HA) content (higher HA: 750mg; lower HA: 250mg) were scanned together with the femurs or lumbar spines each time. We established cross-sectional images of the distal femurs or lumbar spines to perform a three-dimensional histomorphometric analysis of the trabecular bone [31, 87-88, 90-92].

The selected region of interest (ROI) for calculating trabecular bone of distal femur was a 0.72 mm (90 cross-sections) length of the metaphyseal primary and secondary spongiosa, originating 0.24 mm (30 cross-sections) above the epiphyseal growth plate and extending proximally (Fig. 5) [31, 87-88, 90-92]. We analyzed the parameters of the cortical bone in the middle of femoral diaphysis.

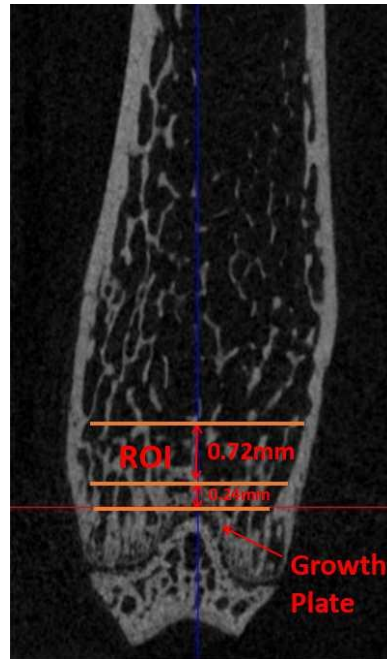


**Figure 5: Selected region of interest (ROI) of distal femur by  $\mu$ CT.**

ROI: The area was a 0.72-mm length, starting 0.24 mm from the lowest growth plate in order to include primary and secondary spongiosa.

The region of interest (ROI round) for calculating trabecular bone of lumbar spine was a cylinder (round) at each slice with a diameter of 0.8mm which was above and beneath respective endplate of each vertebral body, excluding the cortical bone (Fig. 6) [31, 87-88, 90-92].

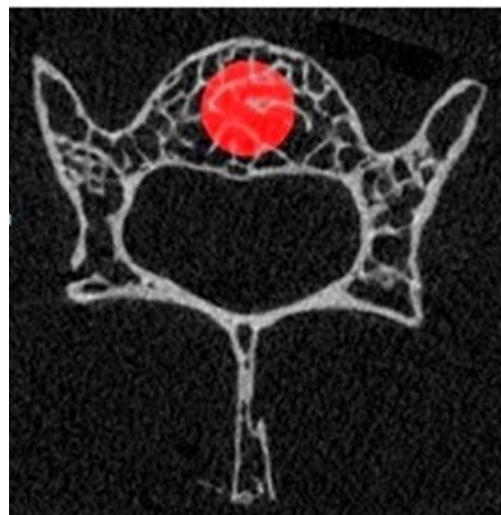


**Figure 6: Selected region of interest (ROI) of lumbar spine by  $\mu$ CT.**

ROI round: The area was a cylinder (round) with a diameter of 0.8 mm, and was above and beneath respective endplate of each vertebral body, excluding the cortical bone.

### **2.4 Histomorphometric analysis**

After analysis of  $\mu$ CT, right femurs were fixed in 4% formalin, dehydrated in graded ethanol. Subsequently, right femurs and lumbar spines were embedded in methyl methacrylate. To identify the number and surface of osteoblasts or osteoclasts, 7- $\mu$ m thick undecalcified sections of intact femurs and lumbar spines were stained by using toluidine blue for better visualization of osteoblasts or tartrate resistant acid phosphatase (TRAP) staining for osteoclasts [31, 87, 91-93]. We performed histomorphometric measurements of the two-dimensional parameters of the trabecular bone with OsteoMeasure Software (OsteoMetrics, Inc.) [31, 87, 91-93].

### **2.5 Statistical analysis.**

Numerical data and histograms were expressed as the mean  $\pm$  SD. Two-tailed Student's t-test was performed between two groups and a difference was considered statistically significant with  $P < 0.05$ .

---

### 3. Results

#### 3.1 Influence of C6 deficiency and CD59a knock-out on trabecular bone

##### 3.1.1 Influence of C6 deficiency on trabecular bone

##### **Global deficiency of C6 reduces trabecular bone mass in distal femur from 17-week-old mice**

$\mu$ CT analysis of the distal femoral metaphysis displayed that bone volume/tissue volume (BV/TV), trabecular number (Tb.N), and bone mineral density (BMD) from C6-deficient mice were significantly lower respectively by 44% ( $P<0.001$ ), 42% ( $P<0.001$ ) and 40% ( $P<0.001$ ) than those from WT littermates at 17 weeks of age (Fig. 7A-C, 7F). Trabecular separation (Tb.Sp) from 17-week-old C6-deficient mice was significantly higher by 29% ( $P<0.001$ ) (Fig. 7E).

In contrast to bone phenotype in 17-week-old mice, BV/TV, Tb.N, Tb.Sp, and BMD in the distal femur were not significantly different between C6-deficient and WT mice at 34 weeks of age (Fig. 7A-F), whereas tissue mineral density (TMD) from 34-week-old C6-deficient mice was significantly lower by 13.5% ( $P=0.003$ ) (Fig. 7G).

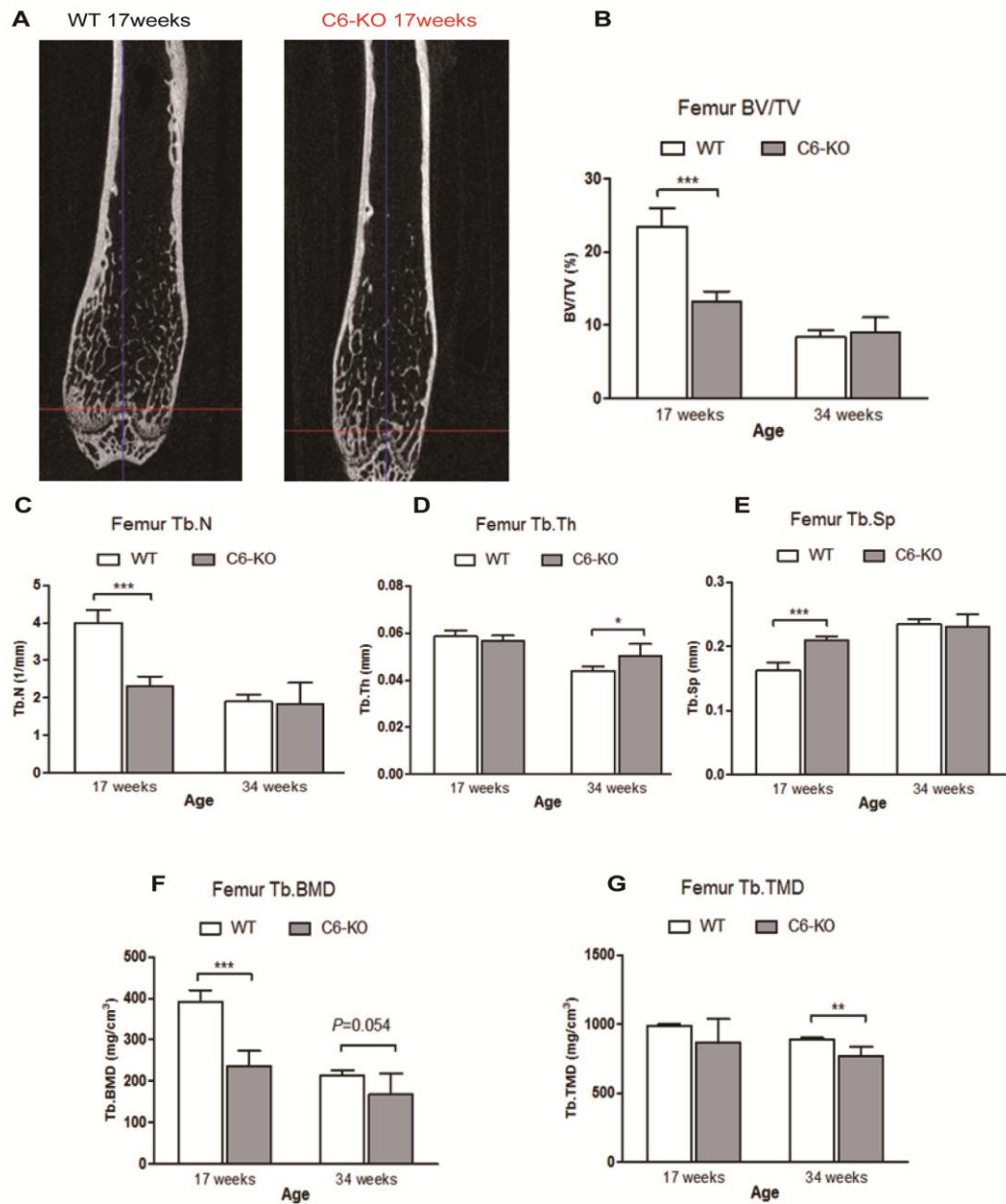


**Figure 7: Low bone mass and bone mineral density (BMD) of trabecular bone in femur from 17-week-old C6-deficient (KO) mice.** (A) Representative  $\mu$ CT images of distal femurs from C6-deficient and WT (C6-sufficient) mice at 17 weeks of age. (B-G) Quantitative  $\mu$ CT analyses of bone volume/tissue volume (BV/TV) (B), trabecular number (Tb.N) (C), trabecular thickness (Tb.Th) (D), trabecular separation (Tb.Sp) (E), BMD (F), and tissue mineral density (TMD) (G) in trabecular bone in distal femurs are shown. All data are mean  $\pm$  SD.  $n = 5-8$  for each group. \*  $P < 0.05$ , \*\*  $P < 0.01$ , and \*\*\*  $P < 0.001$  by Two-tailed Student's t-test between two groups.



---

**Global deficiency of C6 reduces spinal trabecular bone mass**

Compared with WT littermates, BV/TV of vertebrae from C6-deficient mice decreased significantly by 24% ( $P<0.001$ ) and 26% ( $P=0.002$ ) respectively at both ages (Fig. 8A-B). In addition, Tb.N of vertebrae from C6-deficient mice also significantly decreased at both ages by 16% ( $P=0.01$ ) and 23% ( $P<0.001$ ) respectively (Fig. 8C). Trabecular thickness (Tb.Th) and TMD were significantly lower at 17 weeks of age ( $P=0.011$ ;  $P=0.007$ , respectively), but not changed at 34 weeks of age (Fig. 8D, and 8G). Although BMD of vertebrae from C6-deficient mice decreased by 26% and 24% respectively at both ages compared to WT mice, it reached no statistical significance ( $P=0.138$ ;  $P=0.092$ , respectively) (Fig. 8F).

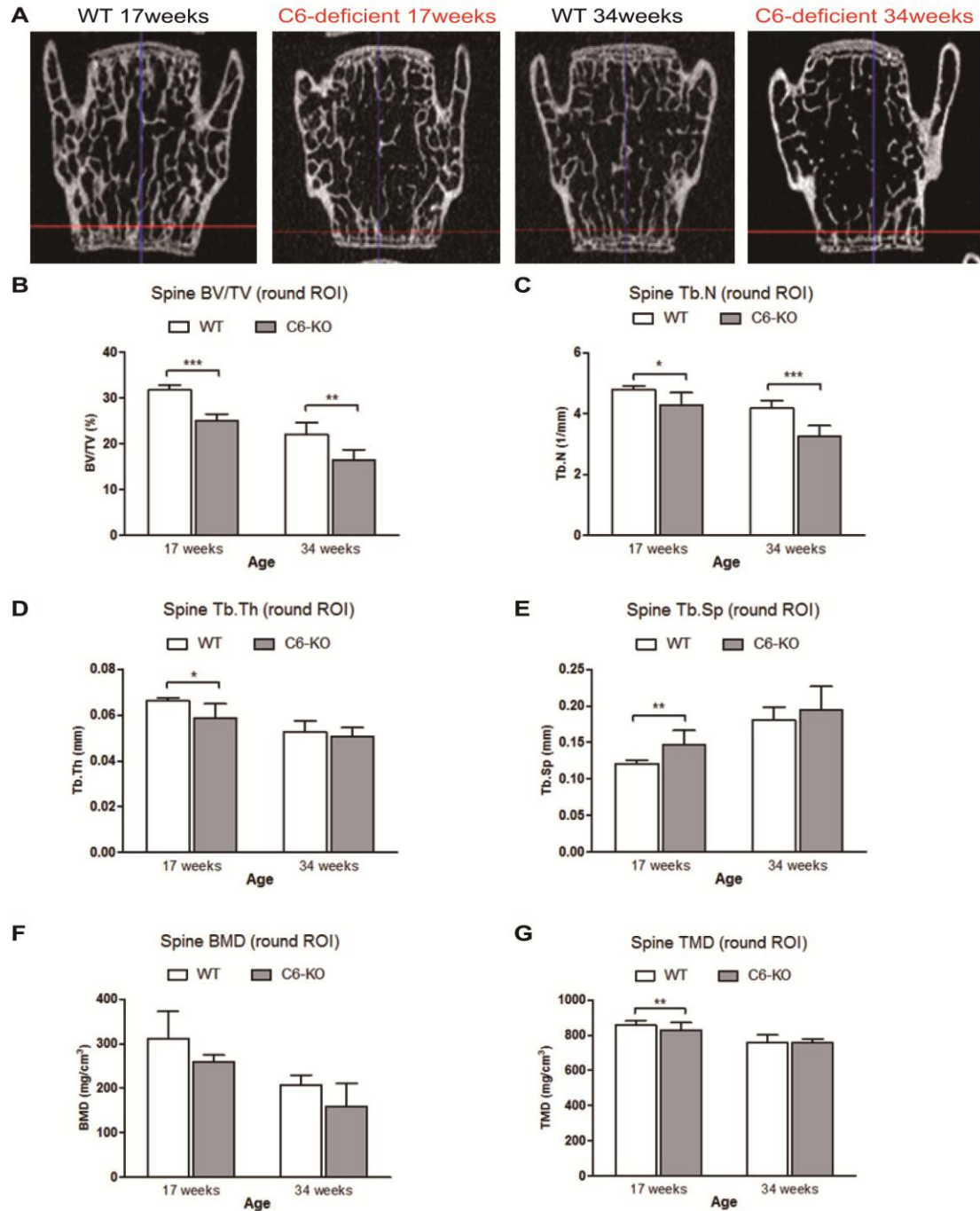


**Figure 8: Decreased bone mass of trabecular bone in spine (round ROI) from C6-deficient (KO) mice.** (A) Representative micro-CT images of lumbar spines from C6-deficient and WT (C6-sufficient) mice at 17 and 34 weeks of age. (B-G) Quantitative  $\mu$ CT analyses of bone volume/tissue volume (BV/TV) (B), trabecular number (Tb.N) (C), trabecular thickness (Tb.Th) (D), trabecular separation (Tb.Sp) (E), bone mineral density (BMD) (F), and tissue mineral density (TMD) (G) in the trabecular bone of vertebral body are shown.

---

### 3.1.2 Global deficiency of C6 increases osteoclast surface of distal femur and spine

To obtain insight the effect of C6 on bone remodeling, histomorphometric analysis displayed that the osteoclast surface per bone surface (Oc.S/BS) of femur from C6-deficient mice was significantly higher by 28% ( $P=0.009$ ) and 43% ( $P=0.008$ ) respectively than that from WT mice at two ages (Fig. 9A, C). In addition, although the number of osteoclasts per bone perimeter (N.Oc/B.Pm) increased significantly by 34% ( $P=0.002$ ) in C6-deficient mice at 34 weeks of age compared to WT mice, it increased by 16% at 17 weeks of age without a statistical significance ( $P=0.091$ , Fig. 9A, B).

Of note, histomorphometry of spine from C6-deficient mice significantly displayed a 29% ( $P=0.014$ ) increase in Oc.S/BS at 17 weeks of age, a 63% ( $P=0.005$ ) increase in Oc.S/BS at 34 weeks of age, a 89.5% ( $P<0.001$ ) increase in N.Oc/B.Pm at 17 weeks of age, and a 87.8% ( $P=0.004$ ) increase in N.Oc/B.Pm at 34 weeks of age, compared to WT mice (Fig. 9D-F).

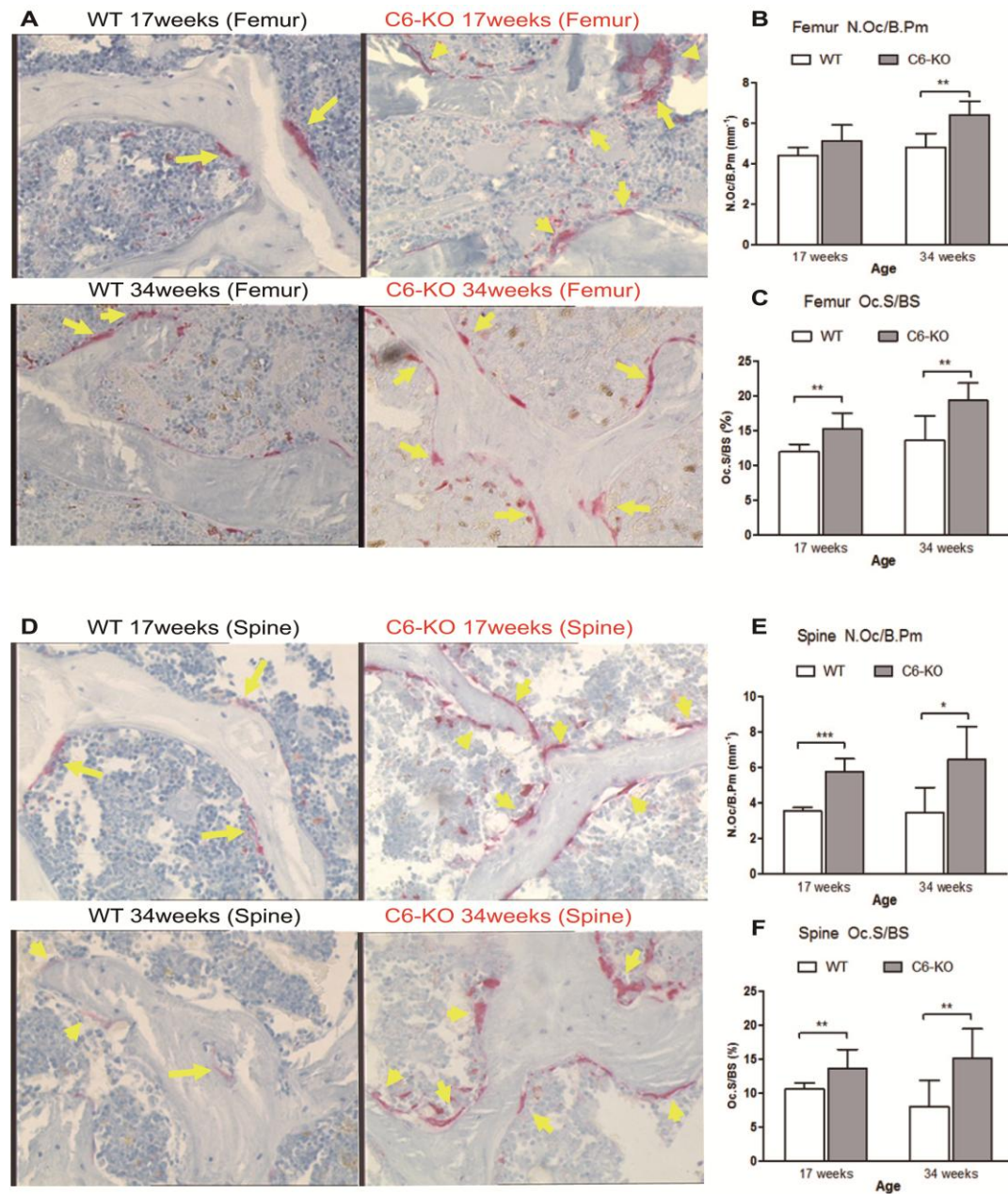


**Figure 9: Increased osteoclast number and surface of trabecular bone from C6-deficient (KO) mice.** (A) Micrographs of tartrate-resistant acid phosphatase (TRAP) staining performed on trabecular bone sections of distal femur from C6-deficient and WT (C6-sufficient) mice at 17 and 34 weeks of age. Dark purple-multinuclear cells were osteoclasts as yellow arrows indicated. (B, C) Quantifications of the number of osteoclasts per bone perimeter (N.Oc/B.Pm) (B) and the osteoclast surface per bone surface (Oc.S/BS) (C) of distal femurs were measured. (D) Representative images of osteoclast counts on trabecular bone sections of vertebral body from C6-KO and WT mice. (E, F) Quantifications of N.Oc/B.Pm (E) and Oc.S/BS (F) in lumbar spines were measured.

### **3.1.3 Global deletion of C6 has no effect on osteoblast number and surface**

With regard to osteoblast number and surface, there were no significantly alterations in N.Ob/B.Pm and Ob.S/BS of femur between C6-deficient and WT mice at two ages (Fig. 10A-C). In addition, N.Ob/B.Pm and Ob.S/BS did not significantly change in C6-deficient mice compared to WT mice at two ages (Fig. 10D-F).

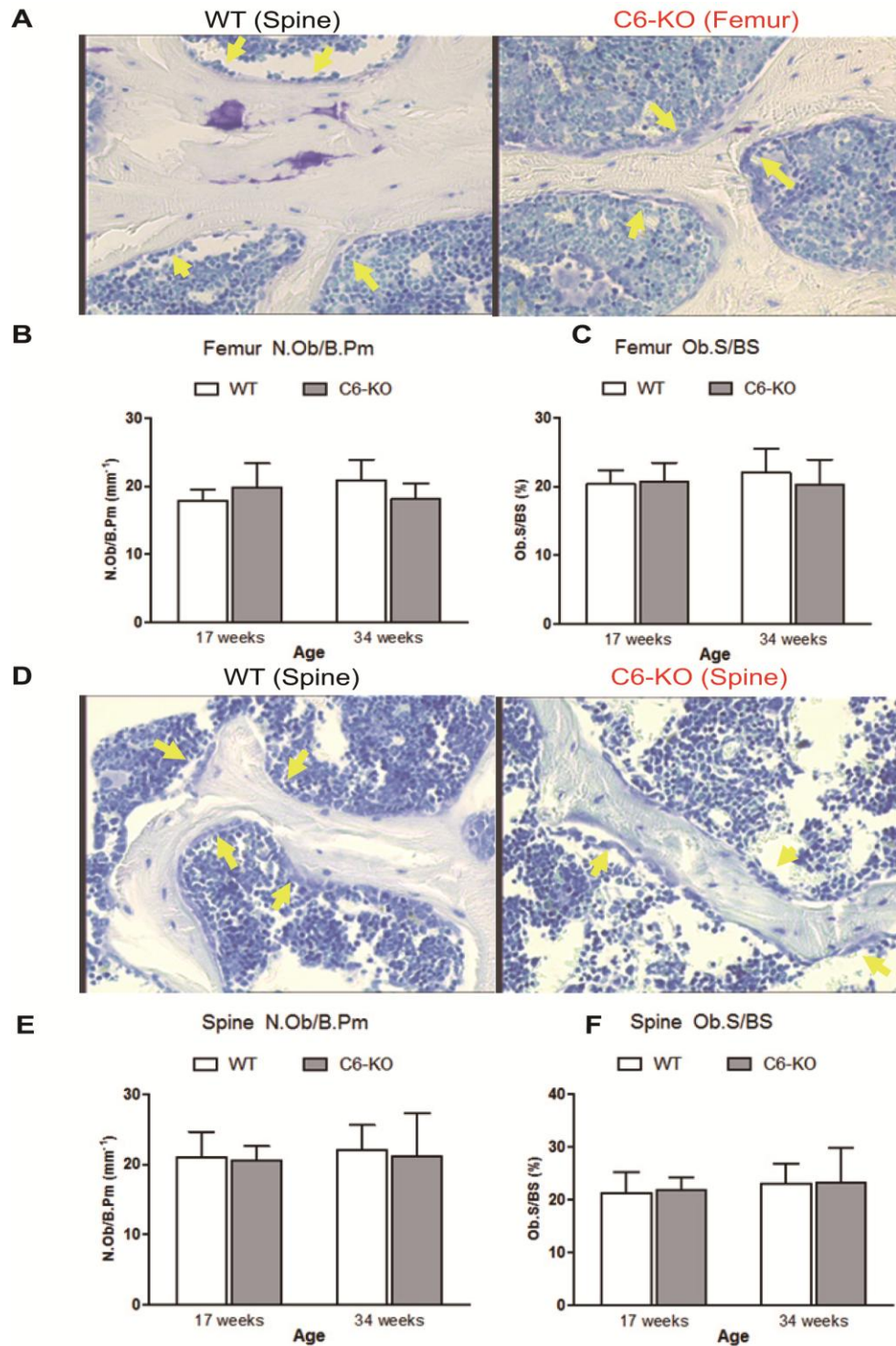


**Figure 10: Unchanged osteoblast number and surface on trabecular bone from C6-deficient (KO) mice.** (A) Micrographs of osteoblast counts on trabecular bone sections of distal femur from C6-KO and WT (C6-sufficient) mice. Light blue cuboid cells continuously at the outer border of bone tissues were osteoblasts as yellow arrows indicated. (B, C) Quantifications of the number of osteoblasts per bone perimeter (N.Ob/B.Pm) (B) and the osteoblast surface per bone surface (Ob.S/BS) (C) in distal femurs were measured. (D) Representative images of osteoblast counts on trabecular bone sections of vertebral body from C6-KO and WT mice. (E, F) Quantifications of N.Ob/B.Pm (E) and Ob.S/BS (F) in lumbar spines were measured.



---

### 3.1.4 Influence of CD59a deficiency on trabecular bone

#### **Global deletion of CD59a reduces trabecular bone mass of distal femur in 17-week-old mice**

$\mu$ CT analysis of the distal femur displayed that trabecular BMD and TMD from CD59a-deficient mice were significantly lower respectively by 28% ( $P<0.001$ ) and 9% ( $P<0.001$ ) than those from WT mice at 17 weeks of age (Fig. 11A-C). Similarly, BV/TV, Tb.N, and Tb.Th of CD59a-deficient mice were significantly lower by 36% ( $P<0.001$ ), 21% ( $P=0.001$ ), and 19% ( $P=0.001$ ) respectively than those of WT mice at 17 weeks of age (Fig. 11D-F), while Tb.Sp of CD59a-deficient mice was significantly higher by 13% ( $P=0.006$ ; Fig. 11G).

However, BMD, TMD, BV/TV, Tb.N, Tb.Th, and Tb.Sp in the trabecular region of distal femur were not significantly different between CD59a-deficient and WT mice at 34 weeks of age (Fig. 11A-G).

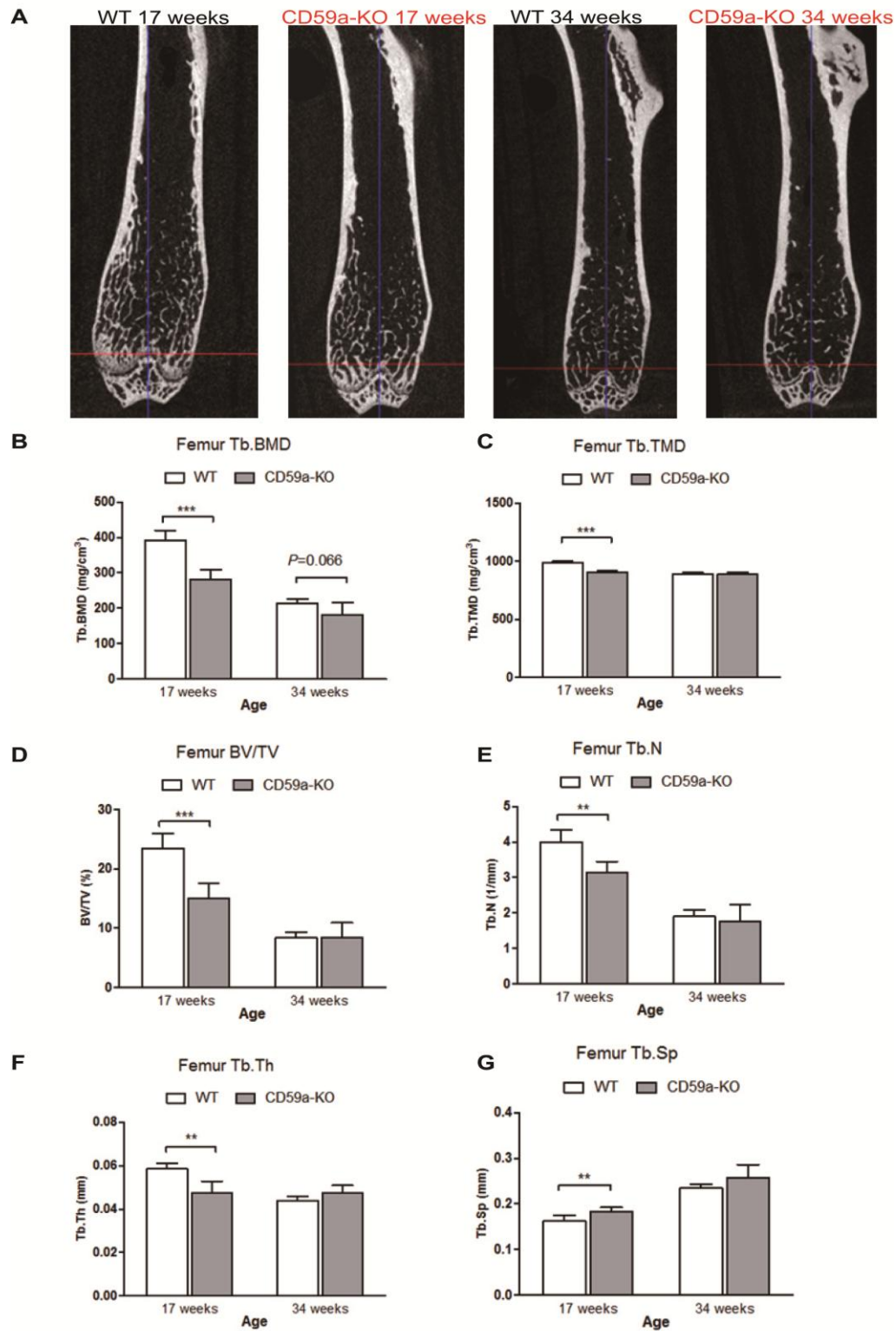


**Figure 11: Low BMD and bone mass of trabecular bone in femur from 17-week-old CD59a-knockout (KO) mice.** Representative  $\mu$ CT images of distal femurs from CD59a-KO and WT mice at two ages. (B-G) Quantitative  $\mu$ CT analyses of bone mineral density (BMD) (B), tissue mineral density (TMD) (C), bone volume/tissue volume (BV/TV) (D), trabecular number (Tb.N) (E), trabecular thickness (Tb.Th) (F), and trabecular separation (Tb.Sp) (G) in the trabecular bone of distal femurs are shown.



---

**Global deletion of CD59a has no effect on trabecular bone of spine**

$\mu$ CT analysis of trabecular bone in spine (round ROI) revealed that BMD, TMD, BV/TV, and Tb.Sp were not significantly different between CD59a-deficient and WT mice at 17 weeks of age (Fig. 12A-D, 12G). Strikingly, Tb.N of spine from CD59a-deficient mice increased significantly by 11% ( $P=0.013$ ) compared to WT mice (Fig. 12E), but Tb.Th decreased significantly 7.6% ( $P=0.009$ ) (Fig. 12F).

In addition, TMD, BV/TV, Tb.N, Tb.Th, and Tb.Sp of spine were not significantly different between CD59a-deficient and WT mice at 34 weeks of age (Fig. 12D-H). However, BMD of spine from CD59a-deficient mice increased significantly by 15% ( $P=0.015$ ) compared to WT mice at 34 weeks of age (Fig. 12B).

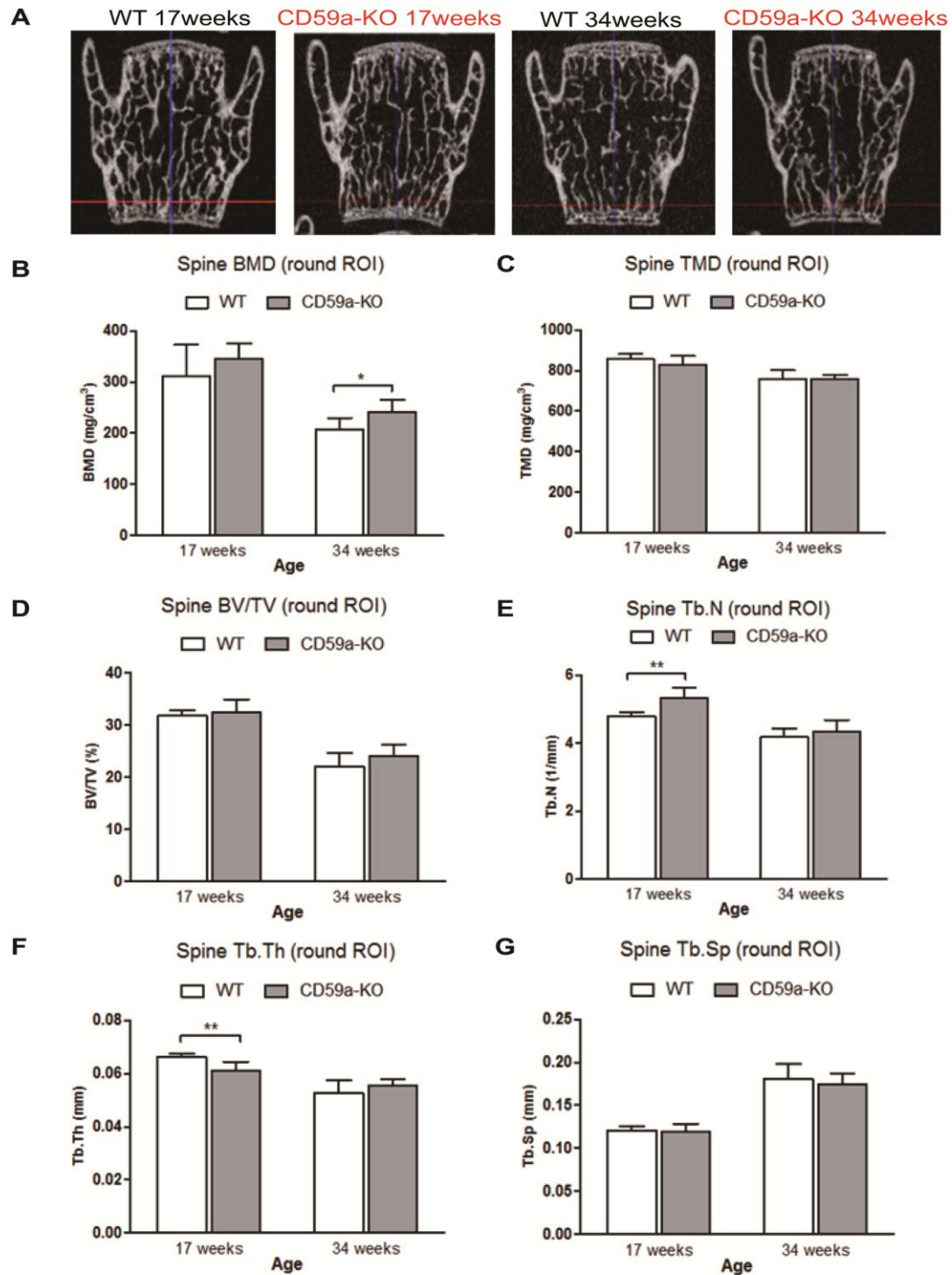


**Figure 12: Unchanged bone mass of spine trabecular bone (round ROI) in CD59a-KO mice.**

(A) Representative  $\mu$ CT images of lumbar spines from CD59a-KO and WT mice at two ages. (B-G) Quantitative  $\mu$ CT analyses of bone mineral density (BMD) (B), tissue mineral density (TMD) (C), bone volume/tissue volume (BV/TV) (D), trabecular number (Tb.N) (E), trabecular thickness (Tb.Th) (F), and trabecular separation (Tb.Sp) (G) in the trabecular bone of vertebral body are shown.

---

### **3.1.5 Global deletion of CD59a in mice increases the number of osteoclasts in femur but not in spine**

Histomorphometric analyses were performed that N.Oc/B.Pm of femur from CD59a-deficient mice was significantly higher by 31% ( $P=0.001$ ) and 29% ( $P=0.005$ ) than that from WT mice at two ages (Fig. 13A-B). Furthermore, compared to WT mice, Oc.S/BS increased by 30% ( $P=0.006$ ) in CD59a-deficient mice at 17 weeks of age, but was not significantly changed ( $P=0.185$ ) at 34 weeks of age (Fig. 13A-C).

Of note, there were no significant differences in N.Oc/B.Pm and Oc.S/BS of spine from CD59a-deficient and WT mice at both ages (Fig. 13D-F).

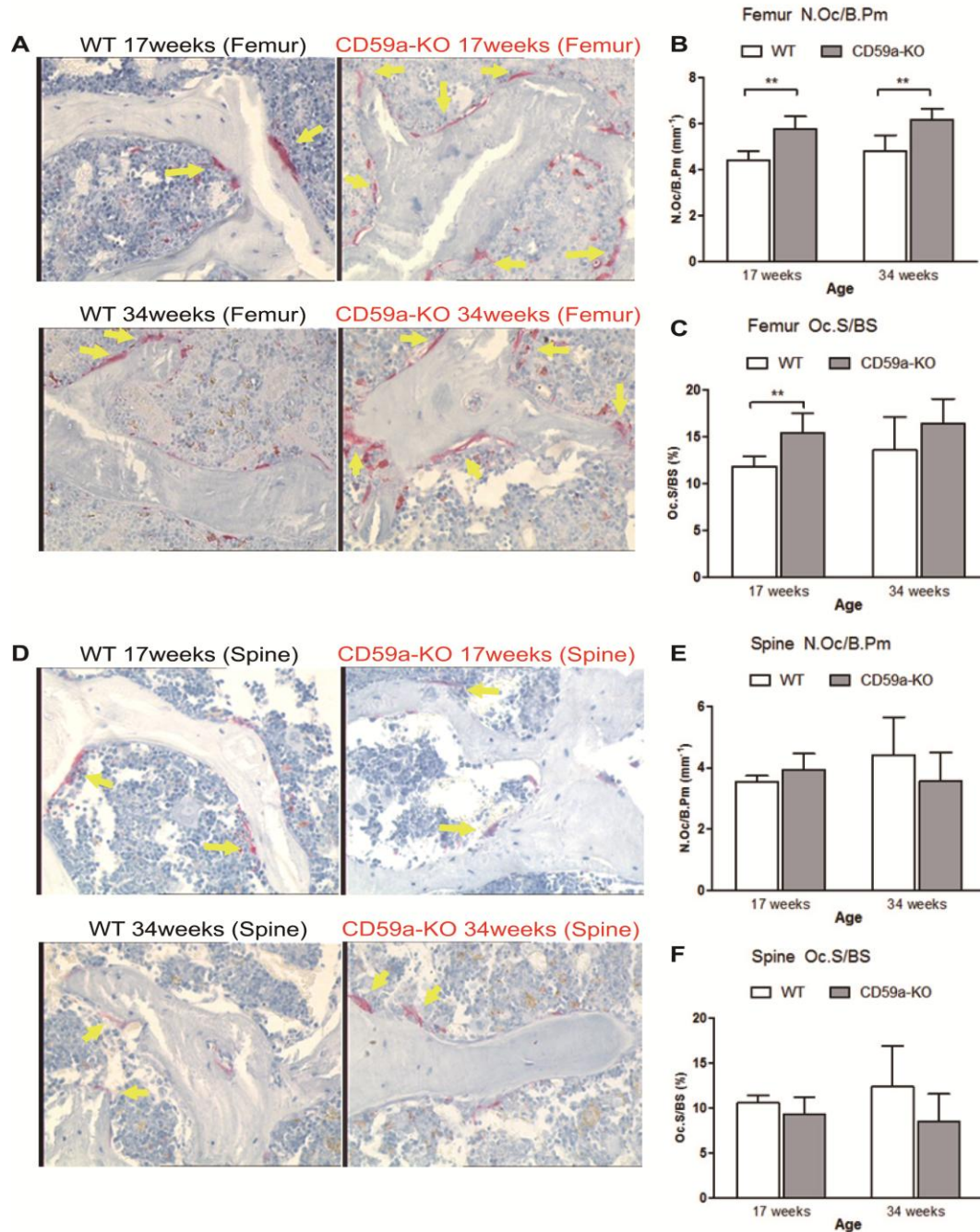


**Figure 13: Decreased osteoclasts number of trabecular bone from CD59a-KO mice.** (A) Micrographs of osteoclasts on trabecular bone sections of distal femur from CD59a-KO and WT mice at two ages. (B, C) Quantifications of the number of osteoclasts per bone perimeter (N.Oc/B.Pm) (B) and the osteoclast surface per bone surface (Oc.S/BS) (C) of distal femurs were measured. (D) Representative images of osteoclasts on trabecular bone sections of vertebral body were shown. (E, F) Quantifications of N.Oc/B.Pm (E) and Oc.S/BS (F) of lumbar spines were measured.

### **3.1.6 Global deficiency of CD59a has no effect on osteoblast number and surface**

In contrast to the pronounced effect on osteoclast number, there were no significant alterations in N.Ob/B.Pm and Ob.S/BS of femur (Fig. 14A-C) or spine (Fig. 14D-F) between CD59a-deficient and WT mice at both ages.

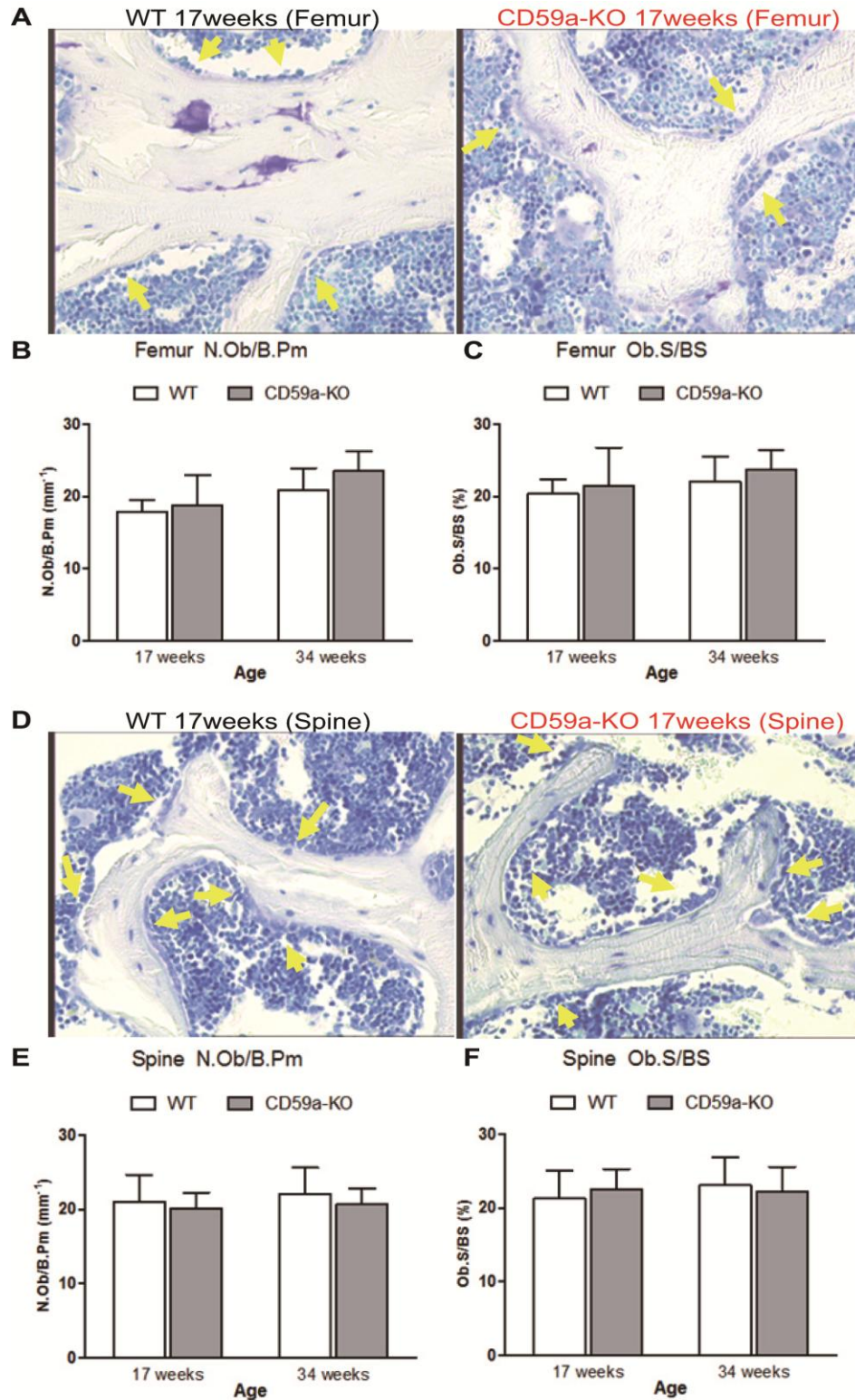


**Figure 14: Unchanged osteoblast number and surface of trabecular bone from CD59a-knockout (KO) mice.** (A) Micrographs of osteoblast counts on trabecular bone sections of distal femur. (B, C) Quantifications of the number of osteoblasts per bone perimeter (N.Ob/B.Pm) (B) and the osteoblast surface per bone surface (Ob.S/BS) (C) of distal femurs were measured. (D) Representative images of osteoblast counts on trabecular bone sections of vertebral body. (E, F) Quantifications of N.Ob/B.Pm (E) and Ob.S/BS (F) of lumbar spines were measured.



### 3.2 Influence of C6-deficiency and CD59a knock-out on cortical bone

#### 3.2.1 Global deletion of C6 decreases mineral density of cortex in femur from 34-week-old mice, with no alterations in cortical thickness

$\mu$ CT analysis of mid-femoral cortex revealed that cortical TMD of C6-deficient mice significantly decreased by 5.2% ( $P=0.001$ ) compared to WT littermates at 34 weeks of age, but did not change at 17 weeks of age (Fig. 15A).

However, deletion of C6 in mice led to no significantly difference in cortical thickness (Ct.Th), compared to WT mice at 17 weeks of age (Fig. 15B-C).

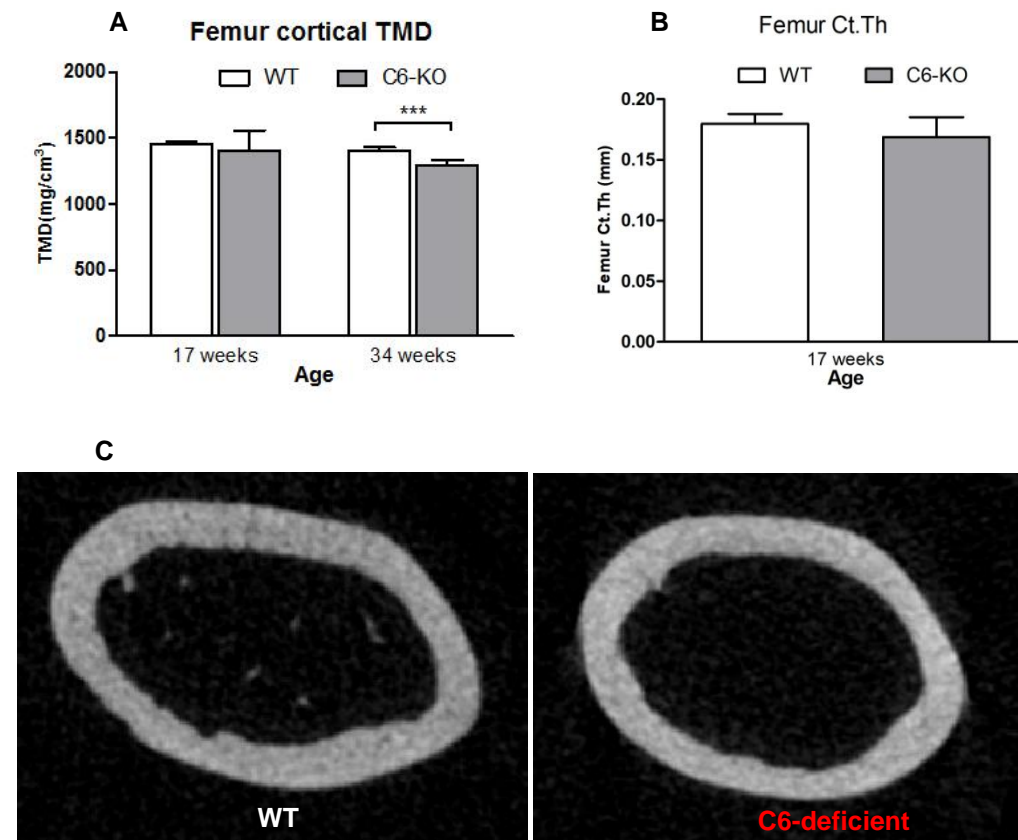


**Figure 15: Low cortical tissue mineral density (TMD) of femur in 34-week-old C6-deficient (C6-KO) mice.** (A, B) Quantitative  $\mu$ CT analyses of cortical TMD (A) and cortical thickness (Ct.Th) (B) of femurs from C6-deficient and WT mice. (C) Representative  $\mu$ CT images of Ct.Th in mid-femur.

### 3.2.2 Global deficiency of C6 has no effect on bending stiffness

With regard to bending stiffness, three-point-bending test of femoral mid-shaft displayed that there were no significant differences in bending stiffness (EI) between C6-deficient and WT mice at 17 weeks of age (Fig. 16A). EI of C6-deficient mice decreased by 15.5%, but that reached no statistical significance ( $P=0.072$ ; Fig. 16A).

Moreover,  $\mu$ CT analysis of bone geometry displayed that moment of inertia in X axis (MOI) of C6-deficient mice significantly decreased by 29% ( $P=0.008$ ) compared to that of WT littermates at 17 weeks of age (Fig. 16B).

However, there were no significant differences in EI and MOI between C6-deficient and WT mice at 34 weeks of age (Fig. 16A, B).

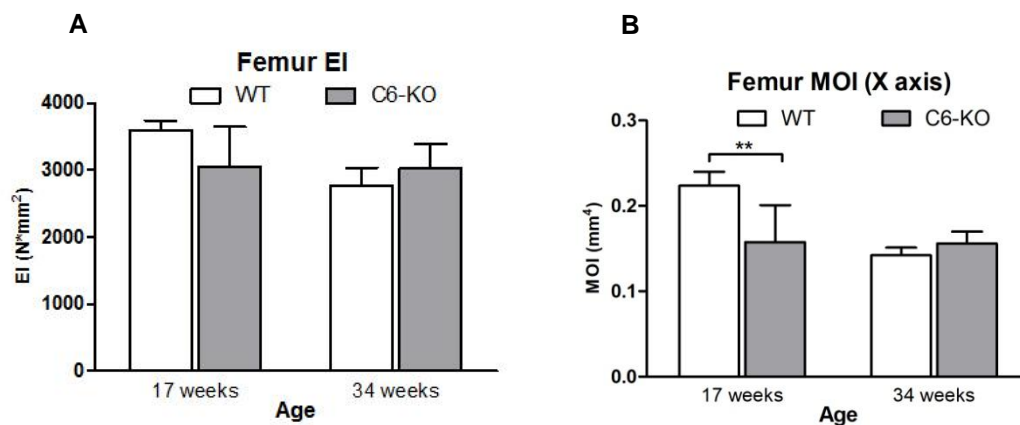


**Figure 16: Unchanged bending stiffness of femur from C6-deficient (KO) mice.**

(A, B) Three-point-bending and quantitative micro-CT analysis of bending stiffness (EI) (A) and moment of inertia in X axis (MOI) (B) in femurs from C6-deficient and WT mice at 17 and 34 weeks of age.

### 3.2.3 Global deletion of CD59a reduces mineral density of cortex in femur, with no alterations in Ct.Th

$\mu$ CT analysis of mid-femoral cortex showed that cortical TMD of CD59a-deficient



mice was significantly decreased compared to WT littermates at both ages. Cortical TMD decreased respectively by 6.6% ( $P<0.001$ ) and 6.9 % ( $P<0.001$ ) (Fig. 17A). Importantly, deletion of CD59 in mice led to no significantly difference in Ct.Th compared to WT mice at both ages (Fig. 17B-C).

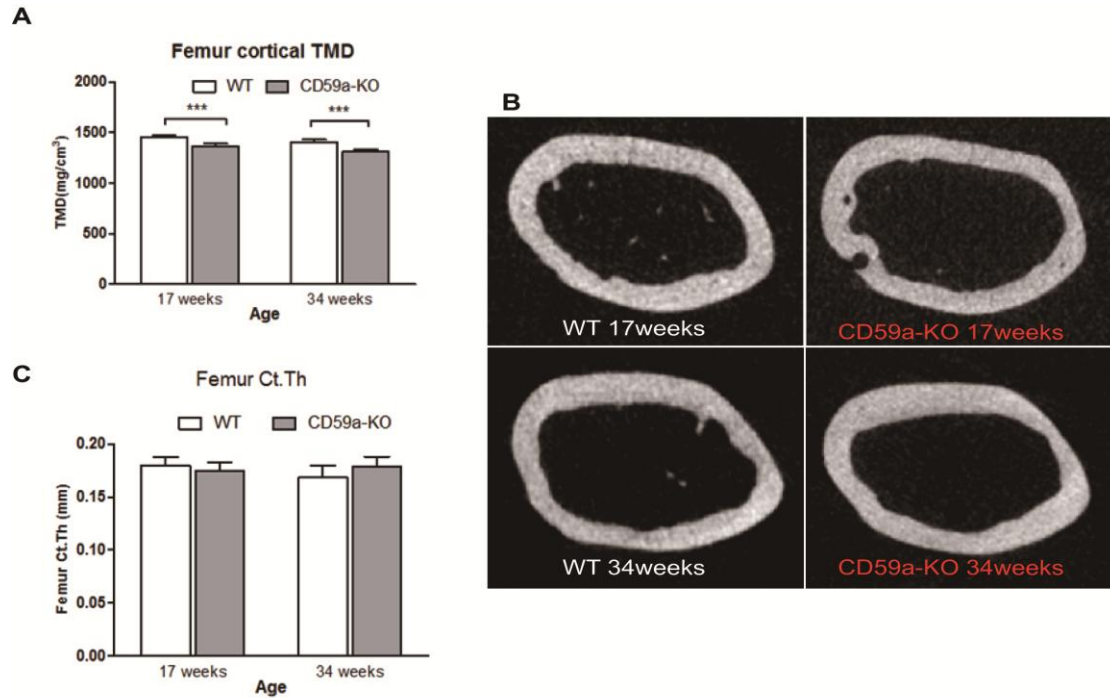


**Figure 17: Low cortical tissue mineral density (TMD) of femur from 17-week-old and 34-week-old CD59a-KO mice.** (A) Quantitative  $\mu$ CT analyses of cortical TMD (A) in mid-femurs from CD59a-KO and WT mice at both ages. (B) Representative  $\mu$ CT images of cortical thickness (Ct.Th) in mid-femurs. (C) Quantitative  $\mu$ CT analysis of Ct.Th in mid-femurs.

### 3.2.4 Increased bending stiffness in CD59a-deficient mice is due to the alterations of bone geometry at 34 weeks of age

Strikingly, 3-point-bending test of femoral midshaft showed that EI of CD59a-deficient mice was higher by 19% ( $P=0.023$ ) than that of WT littermates at 34 weeks of age (Fig. 18A). Moreover, bone geometry analyses from CD59a-deficient mice displayed that MOI, polar moment of inertia (pMOI), total cross-sectional area inside the periosteal envelope (Tt.Ar), and marrow area (Ma.Ar) were all significantly higher respectively by 28% ( $P=0.001$ ), 24% ( $P=0.005$ ), 14% ( $P=0.002$ ) and 16% ( $P=0.006$ ) than those from WT littermates at 34 weeks of age (Fig. 18B-E).

However, there were no significantly differences in EI, MOI, pMOI, Tt.Ar, and Ma.Ar between CD59a-deficient and WT mice at 17 weeks of age (Fig. 18A-E).

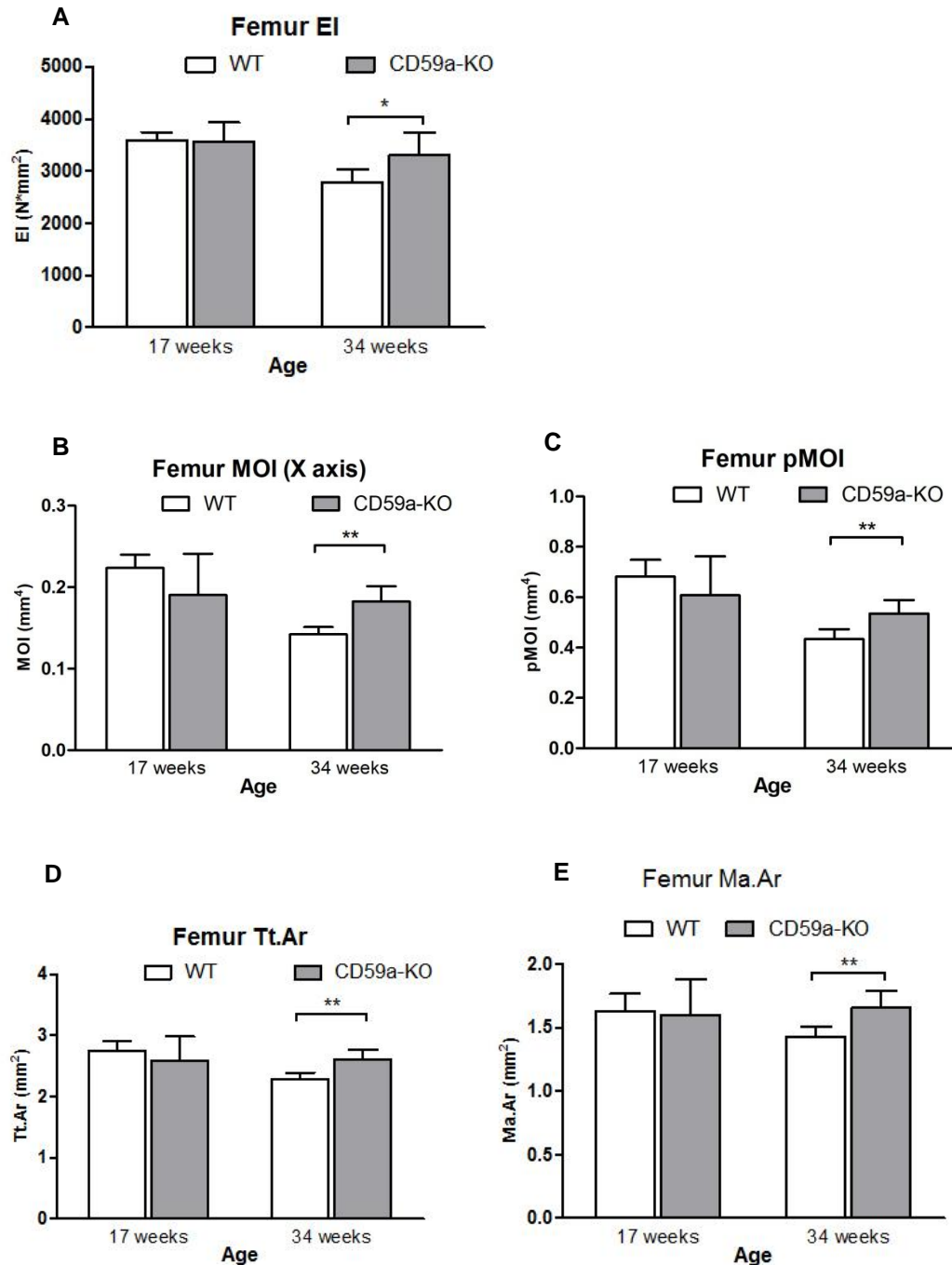


**Figure 18: Increased bending stiffness (EI) and moment of inertia in X axis (MOI) of femur from 34-week-old CD59a-KO mice.** (A-E) Three-point-bending and quantitative  $\mu$ CT analyses of EI (A), MOI (B), polar moment of inertia (pMOI) (C), total cross-sectional area inside the periosteal envelope (Tt.Ar) (D), and marrow area (Ma.Ar) (E) in mid-femurs from CD59a-KO and WT mice at two ages.

---

## 4. Discussion

The aim of this study was to investigate the effects of the terminal complement complex, the MAC, and of the MAC-regulating protein CD59a on bone homeostasis.

### 4.1 The role of CD59a and C6 in bone homeostasis

It was shown previously, that components of the terminal complement system played a role in bone homeostasis and regeneration. Studies in mice lacking the components C3 or C5 revealed that although the mice had no obvious bone phenotype, deficiencies in the terminal complement cascade lead to impaired bone regeneration, as fracture healing in C5-deficient mice was significantly disturbed while C3-knockout mice healed unaffected [94]. Also defective C5aR-signalling was described to influence bone homeostasis and repair. Mice deficient for C5aR1 or C5aR2 displayed significantly increased bone mass in the trabecular compartment of the femur due to different mechanisms: while C5aR1<sup>-/-</sup> led to significantly decreased osteoclast numbers, C5aR2<sup>-/-</sup> resulted in unaltered osteoclast parameters but increased osteoblast numbers. Regarding fracture healing, both C5aR1<sup>-/-</sup> and C5aR2<sup>-/-</sup> displayed impaired healing with more pronounced effects in C5aR1<sup>-/-</sup> [95].

Recently, Wang et al. revealed that low-grade activation of complement system in the joint has a marked impact on the pathogenesis of osteoarthritis [38]: The authors found that synovial membranes of osteoarthritis patients had higher levels of complement effectors and lower levels of complement inhibitors than those of healthy individuals. Moreover, mice lacking CD59a, an inhibitor of MAC, displayed aggravated experimental osteoarthritis, whereas in mice lacking C6, an essential component of MAC, experimental osteoarthritis was attenuated. However, little is known on the role of complement system, especially the MAC, in skeletal homeostasis and integrity.

To analyze the role of the essential MAC-component C6 and the MAC regulatory protein CD59a in the regulation of bone homeostatic bone structure and in age-related

variations, we analyzed the phenotypes of trabecular and cortical bone in C6-deficient and CD59a-knockout male mice at 17 weeks and 34 weeks ages. The present study showed that the femoral trabecular BMD and bone volume of C6-deficient and CD59a-knock-out mice were lower compared to those of WT mice at 17 weeks of age, but were not changed at 34 weeks of age in either genotype.

With regards to femoral cortex, C6-deficiency had no effect on cortical bone at 17 weeks of age, but led to a significant reduction in cortical mineral density at 34 weeks of age. Global knock-out of CD59a resulted in a significant decrease in cortical mineral density at both 17 and 34 weeks of age. In addition, reduced vertebral bone mass was observed in C6-deficient mice at the two investigated ages, but not in CD59a-deficient mice. One possible explanation for this might be that gene-knockout contributes to site-specific variations in peak bone mass [96-98]. In other knock-out models, the gene knock-out led to reduced bone mass and BMD in long bones but not in the vertebrae [98].

Interestingly, in both C6-deficient and CD59a-knock-out mice, osteopenia was associated with increased osteoclast number and surface in the distal femur and spine, whereas neither group showed changes in osteoblast number and surface. Our findings suggest that CD59a-knock-out induces osteopenia by enhancing bone resorption, which is partly consistent with a recent study by Bloom et al. [48]: The authors found that cortical BMD was significantly lower in CD59a<sup>-/-</sup> mice at 8 and 20 weeks of age [48]. However, in contrast to Bloom et al. who reported increased trabecular bone mass in CD59a<sup>-/-</sup> we found an osteopenic bone phenotype. In an *in vitro* study, Bloom et al. also found that deficiency in CD59a promoted osteoclastogenesis from BM of mice, whereas ALP staining and mineralization were not significantly different between cultures derived from male WT and CD59a<sup>-/-</sup> mice. This study of *ex vivo* cultures supports our *in vivo* results with higher osteoclast numbers and unchanged osteoblast parameters. However, little is known whether MAC influences osteoclasts directly, or indirectly promotes inflammation and further activates RANKL and T cells to enhance osteoclastogenesis.

Because of the crosstalk with the complement system, the coagulation system

might also be a possible link between C6-deficiency and the osteopenic phenotype we observed. C6-deficient rodents are described to have defects in coagulation [99]. Due to formation of the MAC, platelets and endothelial cells are induced to release microparticles which can serve as basis for the generation of thrombin from the prothrombin complex [100]. Others could show decreased bone mass in mice with defective factor VIII-thrombin-protease-activated receptor 1 axis [101]. Also other defects in the coagulation cascade, such as impaired fibrinolysis and ineffective clearance of fibrin matrices, could be linked to conditions associated with osteoporosis and to increased fracture risk [102]. The action of MAC seems to be different under physiological and pathological conditions. While our findings suggest that unchallenged mice lacking the MAC or the MAC-regulator CD59a develop osteopenia, in experimental models of osteoarthritis, C6-deficiency and CD59a had diverging effects. While C6-deficient mice were protected against development of meniscectomy-induced osteoarthritis, CD59a-knock-out mice developed more severe OA compared to wildtype-littermates [38]. The authors also showed that chondrocytes coated with sub-lytic concentrations of MAC express cartilage-degrading enzymes, inflammatory cytokines, among them M-CSF and monocyte chemoattractant protein-1, as well as cyclooxygenase 2. In mice with defective MAC-regulation due to CD59a knock-out, MCP-1 and M-CSF might contribute to the increased osteoclast-numbers we observed.

In case of rheumatoid arthritis, C6-deficiency was reported to attenuate the disease to a low-grade inflammatory state. The authors compared the clinical and histopathological scores of C3aR<sup>-/-</sup>, C5aR<sup>-/-</sup> and C6-deficient mice in a model of collagen and antibody-induced arthritis. They found the scores to be reduced in all mice; however, the percentage of synovial macrophages was significantly reduced in C3aR<sup>-/-</sup> and C5aR<sup>-/-</sup>, but not in C6-deficient animals. Infiltrating neutrophils, however, were significantly reduced in all genotypes. Gene expression analysis revealed a significant reduction of IL-1  $\beta$  in C5aR<sup>-/-</sup> and C6-deficient mice [67].

Together with the findings in OA, the reduction in clinical score, infiltration neutrophils and decreased IL-1  $\beta$ -expression clearly show the rather protective effect

of C6 and therefore MAC-deficiency under degenerative and inflammatory conditions.

Contrasting the rather protective effects of C6-deficiency in various disease models, deletion of CD59a, thus inefficient MAC-regulation, leads to increased susceptibility to complement activation and MAC-mediated injury in various disease models including rheumatoid arthritis, nephritis, renal ischemia reperfusion injury, and encephalomyelitis [66, 103-105], emphasizing the importance of regulated MAC-activation. Apart from the function of MAC-mediated cell lysis, sublytic MAC-concentrations are also able to trigger a pro-inflammatory environment in joints by enhancing the expression of pro-inflammatory cytokines and mediators, such as CCL2, CCL5, and CSF1 [38, 77].

It is already known that the immune system exerts differing effects in the physiological state and under pathological inflammatory condition [106]. Under physiological condition the immune system might protect the bone tissue, whereas in an inflammatory environment, activated immune system aggravates bone destruction by stimulating bone resorption [106]. For example, T-cell-deficient and B-cell-deficient mice under physiological circumstance show decreased bone mass and increased bone resorption [107-108]. In contrast, T-cell deficient mice are resistant to ovariectomy-induced bone loss, concurrent with the resistance of stimulating bone resorption and M-CSF/RANKL-dependent osteoclastogenesis [107].

All above imply that MAC is crucial for the physiological process of skeletal homeostasis, as lacking of MAC-inhibition or inactivation of MAC is not sufficient for maintaining normal homeostatic bone structure.

#### **4.2 Age-related changes and the peak mass in skeletal architecture**

Another finding of the present study was an age-dependent phenotype in both C6-deficient and CD59a-knockout mice. We observed dramatic changes and structural deteriorations in femoral cancellous bone of C6-deficient and CD59a-knock-out mice at 17 weeks of age, but not at 34weeks of age. We consider that age may affect the peak and change of bone mass and BMD in both

gene-deficient and WT mice. Bone loss is not only associated with old age in the mouse but also can arise as a continuous process from early growth at early age with reaching peak point [109, 110-112]. In humans, age-related bone loss (Type II osteoporosis) begins near 40 years of age and progresses linearly at a rate of 0.5 to 1% per year, and declines to nearly 40% of total bone loss at 70 years of age [113-115]. Additionally, the measurement by quantitative computed tomography (QCT) and dual energy X-ray absorptiometry (DXA) showed that the peak BMD in humans was at 10-19 years age [116].

Age-related changes and deteriorations in skeletal mass and architecture in the mouse are similar to those features in human aging [109, 110-112]. Rapid growth in young C57BL/6J mice is accompanied by remarkable increases in body mass, bone size, mineral mass, mechanical properties, and increased bone formation rates [112]. Several authors have systematically and comprehensively reported that age-related changes in trabecular architecture at the distal femur and spine in male and female C57BL/6J mice [109, 110]: Ferguson et al. reported that bone length, mass, and mechanical properties reached mature levels at 12 weeks of age. After 42 weeks, age-related bone loss was represented by decreased bone mass, reduced bone mineralization, diminished whole bone stiffness and energy of protecting fracture [112]; Glatt et al. reported that the peak of trabecular BV/TV in distal femur of male C57BL/6J mice was at between 1 and 2 months of age and decreased subsequently throughout life [109]. Our results showed femoral trabecular BMD, BV/TV, Tb.N, and Tb.Th in WT 34-week-old to be considerably lower compared to those from WT 17-week-old mice. Similar to femurs, the peak of vertebral trabecular BV/TV in male C57BL/6J mice is reached between 1 and 2 months of age and kept constant until 6 months and declines over life [109]. Our findings also displayed vertebral BMD, TMD, BV/TV, Tb.N, Tb.Th of 34-week-old male to be considerably decreased compared to WT 17-week-old mice.

With regard to bending stiffness, two decades ago, calculated results of material property in male C57BL/6J mice showed that the stiffness of femoral mid-diaphysis increased from 29.8 N/mm at 4 weeks to a peak value of 162.8 N/mm at 52 weeks,

and later declined to 115.3 N/mm at 104 weeks [112]. Additionally, Beamer et al. found that bone stiffness of 34-week-old male mice was lower by 5.6% than that of 15-week-old mice, whereas the authors didn't show whether it reached significantly statistic or not [112]. Of note, our finding suggested that the femoral bending stiffness of WT 34-week-old mice was reduced by 23% compared to 17-week-old wild type mice.

In conclusion, our results suggest that complement component C6 and the MAC-regulator CD59a play an essential role in maintaining bone mass and skeletal homeostasis during the physiological process of bone remodeling. The mechanisms behind need to be further investigated.



## 5. Summary

The complement system belongs to the innate immune system, and it usually leads to the body's counterattack against bacteria by controlling microbial threats and eliminating cellular debris. The membrane attack complex (MAC) and the anaphylatoxins C5a and C3a are the major effector components of complement. The complement system has been shown to contribute to the pathogenesis of musculoskeletal conditions such as rheumatoid arthritis and osteoarthritis. However, the focus of previous research was mostly on the complement components C3 and C5, their split products and respective receptors. The role of the terminal complement cascade downstream of C5 on bone homeostasis was investigated to a lesser extent. Therefore, the present thesis explored the role of the terminal complement component, the MAC, as well as the role of the MAC-regulatory protein CD59a in bone homeostasis.

To investigate the role of the essential MAC-component C6 and the MAC-regulatory CD59a in the regulation of homeostatic structure of skeleton with age-related variations, we analyzed the phenotypes of trabecular and cortical bone in C6-deficient and CD59a-knockout male mice at 17 weeks and 34 weeks ages. By performing biomechanical testing,  $\mu$ CT analysis, and histomorphometric measurements in mice, we found that the femoral trabecular BMD and bone volume of C6-deficient and CD59a-knockout mice were lower respectively than those of WT mice at 17 weeks of age, but were unchanged at 34 weeks of age in either genotype. BMD in the spine was less affected. Further evidences showed that in both C6-deficient and CD59a-knock-out mice, osteopenia was associated with increased osteoclast number and surface in the distal femur and spine, whereas neither group showed changes in osteoblast number and surface. With regards to cortical phenotypes, global deletion of C6 decreased mineral density of cortex in femur from 34-week-old mice, with no alterations in bending stiffness. In contrast, global deletion of CD59a reduced mineral density of cortex in femur, with no alterations in cortical

thickness. Of note, raised bending stiffness in CD59a-deficient mice at 34 weeks of age was due to the alterations of bone geometry, the increased moment of inertia (pMOI), total cross-sectional area inside the periosteal envelope (Tt.Ar), and marrow area (Ma.Ar).

In conclusion, our results suggest that complement component C6 and the MAC-regulator CD59a play an essential role in preserving bone mass and skeletal homeostasis. As a lack of MAC-inhibition or inactivation of MAC is not sufficient for maintaining normal homeostatic structure, the data provided in this thesis imply that MAC is involved in skeletal homeostasis.

---

## 6. References

1. Clarke B. Normal bone anatomy and physiology. Clin J Am Soc Nephrol. 2008;Suppl 3:S131-9.
2. Zaidi M. Skeletal remodeling in health and disease. Nat Med. 2007;13(7):791-80
3. Long F. Building strong bones: molecular regulation of the osteoblast lineage. Nat Rev Mol Cell Biol. 2011;13:27-38.
4. Brodsky B, Persikov AV. Molecular structure of the collagen triple helix. Adv Protein Chem. 2005;70:301-339.
5. Anderson HC. Matrix vesicles and calcification. Curr Rheumatol Rep. 2003;5:222-226.
6. Bonewald LF. The amazing osteocyte. J Bone Miner Res. 2011;26:229-238.
7. Manolagas SC. Birth and death of bone cells: basic regulatory mechanisms and implications for the pathogenesis and treatment of osteoporosis. Endocr Rev. 2000;21:115-137.
8. Jilka RL, Weinstein RS, Bellido T, Parfitt AM, Manolagas SC. Osteoblast programmed cell death (apoptosis): modulation by growth factors and cytokines. J Bone Miner Res. 1998;13:793-802.
9. Compton JT, Lee FY. A review of osteocyte function and the emerging importance of sclerostin. J Bone Joint Surg Am. 2014;96:1659-1668.
10. Dallas SL, Prideaux M, Bonewald LF. The osteocyte: an endocrine cell ... and more. Endocr Rev. 2013;34:658-690.
11. Han Y, Cowin SC, Schaffler MB, Weinbaum S. Mechanotransduction and strain amplification in osteocyte cell processes. Proc Natl Acad Sci U S A. 2004;101:16689-16694.
12. Walker, DG. Bone resorption restored in osteopetrotic mice by transplants of normal bone marrow and spleen cells. Science. 1975;190:784-785.
13. Walker, DG. Congenital osteopetrosis in mice cured by parabiotic union with normal siblings. Endocrinology. 1972;91:916-920.

14. Anderson DM, Maraskovsky E, Billingsley WL, Dougall WC, Tometsko ME, Roux ER, Teepe MC, DuBose RF, Cosman D, Galibert L. A homologue of the TNF receptor and its ligand enhance T-cell growth and dendritic-cell function. *Nature*. 1997;390:175-179.
15. Lacey DL, Timms E, Tan HL, Kelley MJ, Dunstan CR, Burgess T, Elliott R, Colombero A, Elliott G, Scully S, Hsu H, Sullivan J, Hawkins N, Davy E, Capparelli C, Eli A, Qian YX, Kaufman S, Sarosi I, Shalhoub V, Senaldi G, Guo J, Delaney J, Boyle WJ. Osteoprotegerin ligand is a cytokine that regulates osteoclast differentiation and activation. *Cell*. 1998;93:165-176.
16. Matsuzaki K, Udagawa N, Takahashi N, Yamaguchi K, Yasuda H, Shima N, Morinaga T, Toyama Y, Yabe Y, Higashio K, Suda T. Osteoclast differentiation factor (ODF) induces osteoclast-like cell formation in human peripheral blood mononuclear cell cultures. *Biochem Biophys Res Commun*. 1998;246:199-204.
17. Wong BR, Josien R, Lee SY, Sauter B, Li HL, Steinman RM, Choi Y. TRANCE (tumor necrosis factor [TNF]-related activation-induced cytokine), a new TNF family member predominantly expressed in T cells, is a dendritic cell-specific survival factor. *J Exp Med*. 1997;186:2075-2080.
18. Wong BR, Rho J, Arron J, Robinson E, Orlinick J, Chao M, Kalachikov S, Cayani E, Bartlett FS 3rd, Frankel WN, Lee SY, Choi Y. TRANCE is a novel ligand of the tumor necrosis factor receptor family that activates c-Jun N-terminal kinase in T cells. *J Biol Chem*. 1997;272:25190-25194.
19. Kong YY, Yoshida H, Sarosi I, Tan HL, Timms E, Capparelli C, Morony S, Oliveira-dos-Santos AJ, Van G, Itie A, Khoo W, Wakeham A, Dunstan CR, Lacey DL, Mak TW, Boyle WJ, Penninger JM. OPGL is a key regulator of osteoclastogenesis, lymphocyte development and lymph-node organogenesis. *Nature*. 1999;397:315-323.
20. Yoshida H, Hayashi S, Kunisada T, Ogawa M, Nishikawa S, Okamura H, Sudo T, Shultz LD, Nishikawa S. The murine mutation osteopetrosis is in the coding region of the macrophage colony stimulating factor gene. *Nature*. 1990;345:442-444.

21. Teitelbaum SL. Bone resorption by osteoclasts. *Science*. 2000;289:1504-1508.
22. Khosla S. Minireview: the OPG/RANKL/RANK system. *Endocrinology*. 2001;142:5050-5055.
23. Whyte MP. Paget's disease of bone and genetic disorders of RANKL/OPG/NF-kappaB signaling. *Ann N Y Acad Sci*. 2006;1068:143-164.
24. Xiong J, Onal M, Jilka RL, Weinstein RS, Manolagas SC, O'Brien CA. Matrix-embedded cells control osteoclast formation. *Nat Med*. 2011;17:1235-1241.
25. Nakashima T, Hayashi M, Fukunaga T, Kurata K, Oh-Hora M, Feng JQ, Bonewald LF, Kodama T, Wutz A, Wagner EF, Penninger JM, Takayanagi H. Evidence for osteocyte regulation of bone homeostasis through RANKL expression. *Nat Med*. 2011;17:1231-1234.
26. Weitzmann MN, Pacifici R. Estrogen deficiency and bone loss: an inflammatory tale. *J Clin Invest*. 2006;116:1186-1194.
27. Clowes JA, Riggs BL, Khosla S. The role of the immune system in the pathophysiology of osteoporosis. *Immunol Rev*. 2005;208:207-227.
28. Zhu LL, Blair H, Cao J, Yuen T, Latif R, Guo L, Tourkova IL, Li J, Davies TF, Sun L, Bian Z, Rosen C, Zallone A, New MI, Zaidi M. Blocking antibody to the  $\beta$ -subunit of FSH prevents bone loss by inhibiting bone resorption and stimulating bone synthesis. *Proc Natl Acad Sci U S A*. 2012;109:14574-14579.
29. Devleta B, Adem B, Senada S. Hypergonadotropic amenorrhea and bone density: new approach to an old problem. *J Bone Miner Metab*. 2004;22:360-364.
30. Sowers MR, Jannausch M, McConnell D, Little R, Greendale GA, Finkelstein JS, Neer RM, Johnston J, Ettinger B. Hormone predictors of bone mineral density changes during the menopausal transition. *J Clin Endocrinol Metab*. 2006;91:1261-1267.
31. Yu B, Chang J, Liu Y, Li J, Kevork K, Al-Hezaimi K, Graves DT, Park NH, Wang CY. Wnt4 signaling prevents skeletal aging and inflammation by inhibiting nuclear factor- $\kappa$ B. *Nat Med*. 2014;20:1009-1017.
32. Ginaldi L, Di Benedetto MC, De Martinis M. Osteoporosis, inflammation and

- 
- ageing. *Immun Ageing*. 2005;2:14.
33. McLean RR. Proinflammatory cytokines and osteoporosis. *Curr Osteoporos Rep*. 2009;7:134-139.
  34. Ashpole NM, Herron JC, Mitschelen MC, Farley JA, Logan S, Yan H, Ungvari Z, Hodges EL, Csiszar A, Ikeno Y, Humphrey MB, Sonntag WE. IGF-1 regulates vertebral bone aging through sex-specific and time-dependent Mechanisms. *J Bone Miner Res*. 2016;31:443-454.
  35. Ricklin D, Hajishengallis G, Yang K, Lambris JD. Complement: a key system for immune surveillance and homeostasis. *Nat Immunol*. 2010;11:785-797.
  36. Leslie M. Immunology. The new view of complement. *Science*. 2012;337:1034-1037.
  37. Ricklin D, Reis ES, Lambris JD. Complement in disease: a defence system turning offensive. *Nat Rev Nephrol*. 2016;12:383-401.
  38. Wang Q, Rozelle AL, Lepus CM, Scanzello CR, Song JJ, Larsen DM, Crish JF, Bebek G, Ritter SY, Lindstrom TM, Hwang I, Wong HH, Punzi L, Encarnacion A, Shamloo M, Goodman SB, Wyss-Coray T, Goldring SR, Banda NK, Thurman JM, Gobezie R, Crow MK, Holers VM, Lee DM, Robinson WH. Identification of a central role for complement in osteoarthritis. *Nat Med*. 2011;17:1674-1679.
  39. Harboe M, Mollnes TE. The alternative complement pathway revisited. *J Cell Mol Med*. 2008;12:1074-1084.
  40. Müller-Eberhard, HJ. The killer molecule of complement. *J Invest Dermatol*. 1985;85:47s-52s.
  41. Morgan BP. The membrane attack complex as an inflammatory trigger. *Immunobiology*. 2016;221:747-751.
  42. Bohana-Kashtan O, Ziporen L, Donin N, Kraus S, Fishelson Z. Cell signals transduced by complement. *Mol Immunol*. 2004;41:583-597.
  43. Coulthard LG, Woodruff TM. Is the complement activation product C3a a proinflammatory molecule? Re-evaluating the evidence and the myth. *J Immunol*. 2015;194:3542-3548.
  44. Nordahl EA, Rydengård V, Nyberg P, Nitsche DP, Mörgelin M, Malmsten M,

- 
- Björck L, Schmidtchen A. Activation of the complement system generates antibacterial peptides. *Proc Natl Acad Sci U S A*. 2004;101:16879-16884.
45. Ignatius A, Schoengraf P, Kreja L, Liedert A, Recknagel S, Kandert S, Brenner RE, Schneider M, Lambris JD, Huber-Lang M. Complement C3a and C5a modulate osteoclast formation and inflammatory response of osteoblasts in synergism with IL-1beta. *J Cell Biochem*. 2011;112:2594-2605.
  46. Ignatius A, Ehrnthaller C, Brenner RE, Kreja L, Schoengraf P, Lisson P, Blakytyn R, Recknagel S, Claes L, Gebhard F, Lambris JD, Huber-Lang M. The anaphylatoxin receptor C5aR is present during fracture healing in rats and mediates osteoblast migration in vitro. *J Trauma*. 2011;71:952-960.
  47. Andrades JA, Nimni ME, Becerra J, Eisenstein R, Davis M, Sorgente N. Complement proteins are present in developing endochondral bone and may mediate cartilage cell death and vascularization. *Exp Cell Res*. 1996;227:208-213.
  48. Bloom AC, Collins FL, Van't Hof RJ, Ryan ES, Jones E, Hughes TR, Morgan BP, Erlandsson M, Bokarewa M, Aeschlimann D, Evans BAJ, Williams AS. Deletion of the membrane complement inhibitor CD59a drives age and gender-dependent alterations to bone phenotype in mice. *Bone*. 2016;84:253-261.
  49. Tu Z, Bu H, Dennis JE, Lin F. Efficient osteoclast differentiation requires local complement activation. *Blood*. 2010;116:4456-4463.
  50. Schiller C, Gruber R, Ho GM, Redlich K, Guber HJ, Katzgraber F, Willheim M, Hoffmann O, Pietschmann P, Peterlik M. Interaction of triiodothyronine with 1alpha,25-dihydroxyvitamin D3 on interleukin-6-dependent osteoclast-like cell formation in mouse bone marrow cell cultures. *Bone*. 1998;22:341-346.
  51. Gao Y, Morita I, Maruo N, Kubota T, Murota S, Aso T. Expression of IL-6 receptor and GP130 in mouse bone marrow cells during osteoclast differentiation. *Bone*. 1998;22:487-493.
  52. Holt DS, Botto M, Bygrave AE, Hanna SM, Walport MJ, Morgan BP. Targeted deletion of the CD59 gene causes spontaneous intravascular hemolysis and hemoglobinuria. *Blood*. 2001;98:442-449.

53. Beurskens FJ, Kuenen JD, Hofhuis F, Fluit AC, Robins DM, Van Dijk H. Sexlimited protein: in vitro and in vivo functions. *Clin Exp Immunol.* 1999;116:395-400.
54. Schett G, David JP. The multiple faces of autoimmune-mediated bone loss. *Nat Rev Endocrinol.* 2010;6:698-706.
55. Grahnmö L, Andersson A, Nurkkala-Karlsson M, Stubelius A, Lagerquist MK, Svensson MN, Ohlsson C, Carlsten H, Islander U. Trabecular bone loss in collagen antibody-induced arthritis. *Arthritis Res Ther.* 2015;17:189.
56. Forsblad D'Elia H, Larsen A, Waltbrand E, Kvist G, Mellström D, Saxne T, Ohlsson C, Nordborg E, Carlsten H. Radiographic joint destruction in postmenopausal rheumatoid arthritis is strongly associated with generalised osteoporosis. *Ann Rheum Dis.* 2003;62:617-623.
57. Ruddy S, Colten HR. Rheumatoid arthritis: biosynthesis of complement proteins by synovial tissues. *N Engl J Med.* 1974;290:1284-1288.
58. Hietala MA, Jonsson IM, Tarkowski A, Kleinau S, Pekna M. Complement deficiency ameliorates collagen-induced arthritis in mice. *J Immunol.* 2002;169:454-459.
59. Helmy KY, Katschke KJ Jr, Gorgani NN, Kljavin NM, Elliott JM, Diehl L, Scales SJ, Ghilardi N, van Lookeren Campagne M. CR1g: a macrophage complement receptor required for phagocytosis of circulating pathogens. *Cell.* 2006;124:915-927.
60. Katschke KJ Jr, Helmy KY, Steffek M, Xi H, Yin J, Lee WP, Gribling P, Barck KH, Carano RA, Taylor RE, Rangell L, Diehl L, Hass PE, Wiesmann C, van Lookeren Campagne M. A novel inhibitor of the alternative pathway of complement reverses inflammation and bone destruction in experimental arthritis. *J Exp Med.* 2007;204:1319-1325.
61. Goodfellow RM, Williams AS, Levin JL, Williams BD, Morgan BP. Soluble complement receptor one (sCR1) inhibits the development and progression of rat collagen-induced arthritis. *Clin Exp Immunol.* 2000;119:210-206.
62. Dreja H, Annenkov A, Chernajovsky Y. Soluble complement receptor 1 (CD35)



- 
- delivered by retrovirally infected syngeneic cells or by naked DNA injection prevents the progression of collagen-induced arthritis. *Arthritis Rheum.* 2000;43:1698-1709.
63. Linton SM, Williams AS, Dodd I, Smith R, Williams BD, Morgan BP. Therapeutic efficacy of a novel membrane - targeted complement regulator in antigen - induced arthritis in the rat. *Arthritis Rheum.* 2000;43:2590-2597.
  64. Wang Y, Rollins SA, Madri JA, Matis LA. Anti-C5 monoclonal antibody therapy prevents collagen-induced arthritis and ameliorates established disease. *Proc Natl Acad Sci U S A.* 1995;92:8955-8959.
  65. Wang Y, Kristan J, Hao L, Lenkoski CS, Shen Y, Matis LA. A role for complement in antibody-mediated inflammation: C5-deficient DBA/1 mice are resistant to collagen-induced arthritis. *J Immunol.* 2000;164:4340-4347.
  66. Williams AS, Mizuno M, Richards PJ, Holt DS, Morgan BP. Deletion of the gene encoding CD59a in mice increases disease severity in a murine model of rheumatoid arthritis. *Arthritis Rheum.* 2004;50:3035-3044.
  67. Banda NK, Hyatt S, Antonioli AH, White JT, Glogowska M, Takahashi K, Merkel TJ, Stahl GL, Mueller-Ortiz S, Wetsel R, Arend WP, Holers VM. Role of C3a receptors, C5a receptors, and complement protein C6 deficiency in collagen antibody-induced arthritis in mice. *J Immunol.* 2012;188:1469-1478.
  68. Robinson WH, Lepus CM, Wang Q, Raghu H, Mao R, Lindstrom TM, Sokolove J. Low-grade inflammation as a key mediator of the pathogenesis of osteoarthritis. *Nat Rev Rheumatol.* 2016;12:580-592.
  69. Rosado CJ, Buckle AM, Law RH, Butcher RE, Kan WT, Bird CH, Ung K, Browne KA, Baran K, Bashtannyk-Puhlovich TA, Faux NG, Wong W, Porter CJ, Pike RN, Ellisdon AM, Pearce MC, Bottomley SP, Emsley J, Smith AI, Rossjohn J, Hartland EL, Voskoboinik I, Trapani JA, Bird PI, Dunstone MA, Whisstock JC. A common fold mediates vertebrate defense and bacterial attack. *Science.* 2007;317:1548-1551.
  70. Tschopp J, Masson D, Stanley KK. Structural/functional similarity between proteins involved in complement- and cytotoxic T- lymphocyte-mediated

- cytolysis. *Nature*. 1986;322:831-844.
71. Cooke TD, Bennett EL, Ohno O. The deposition of immunoglobulins and complement in osteoarthritic cartilage. *Int Orthop*. 1980;4:211-217.
72. Corvetta A, Pomponio G, Rinaldi N, Luchetti MM, Di Loreto C, Stramazzotti D. Terminal complement complex in synovial tissue from patients affected by rheumatoid arthritis, osteoarthritis and acute joint trauma. *Clin Exp Rheumatol*. 1992;10:433-438.
73. Glasson SS, Askew R, Sheppard B, Carito B, Blanchet T, Ma HL, Flannery CR, Peluso D, Kanki K, Yang Z, Majumdar MK, Morris EA. Deletion of active ADAMTS5 prevents cartilage degradation in a murine model of osteoarthritis. *Nature*. 2005;434:644-648.
74. Stanton H, Rogerson FM, East CJ, Golub SB, Lawlor KE, Meeker CT, Little CB, Last K, Farmer PJ, Campbell IK, Fourie AM, Fosang AJ. ADAMTS5 is the major aggrecanase in mouse cartilage in vivo and in vitro. 2005;434:648-652.
75. Sofat N. Analysing the role of endogenous matrix molecules in the development of osteoarthritis. *Int J Exp Pathol*. 2009;90:463-479.
76. Attur M, Al-Mussawir HE, Patel J, Kitay A, Dave M, Palmer G, Pillinger MH, Abramson SB. Prostaglandin E2 exerts catabolic effects in osteoarthritis cartilage: evidence for signaling via the EP4 receptor. *J Immunol*. 2008;181:5082-5088.
77. Scanzello CR, McKeon B, Swaim BH, DiCarlo E, Asomugha EU, Kanda V, Nair A, Lee DM, Richmond JC, Katz JN, Crow MK, Goldring SR. Synovial inflammation in patients undergoing arthroscopic meniscectomy: molecular characterization and relationship to symptoms. *Arthritis Rheum*. 2011;63:391-400.
78. Badea TD, Park JH, Soane L, Niculescu T, Niculescu F, Rus H, Shin ML. Sublytic terminal complement attack induces c-fos transcriptional activation in myotubes. *J Neuroimmunol*. 2003;142:58-66.
79. Rus HG, Niculescu F, Shin ML. Sublytic complement attack induces cell cycle in oligodendrocytes. *J Immunol*. 1996;156:4892-4900.
80. Pihlstrom BL, Michalowicz BS, Johnson NW. Periodontal diseases. *Lancet*.

- 
- 2005;366:1809-1820.
81. Hajishengallis G. Periodontitis: from microbial immune subversion to systemic inflammation. *Nat Rev Immunol.* 2015;15:30-44.
  82. Kebschull M, Demmer RT, Papapanou PN. "Gum bug, leave my heart alone!"--epidemiologic and mechanistic evidence linking periodontal infections and atherosclerosis. *J Dent Res.* 2010;89:879-902.
  83. Hajishengallis G, Hajishengallis E, Kajikawa T, Wang B, Yancopoulou D, Ricklin D, Lambris JD. Complement inhibition in pre-clinical models of periodontitis and prospects for clinical application. *Semin Immunol.* 2016;28:285-291.
  84. Patters MR, Niekrash CE, Lang NP. Assessment of complement cleavage in gingival fluid during experimental gingivitis in man. *J Clin Periodontol.* 1989;16:33-37.
  85. Niekrash CE, Patters MR. Simultaneous assessment of complement components C3, C4, and B and their cleavage products in human gingival fluid. II. Longitudinal changes during periodontal therapy. *J Periodontal Res.* 1985;20:268-275.
  86. Miwa T, Zhou L, Hilliard B, Molina H, Song WC. Crry, but not CD59 and DAF, is indispensable for murine erythrocyte protection in vivo from spontaneous complement attack. *Blood.* 2002;99:3707-3716.
  87. Rapp AE, Bindl R, Recknagel S, Erbacher A, Müller I, Schrezenmeier H, Ehrnthaller C, Gebhard F, Ignatius A. Fracture Healing Is Delayed in Immunodeficient NOD/scid- IL2R $\gamma$ null Mice. *PLoS One.* 2016;11:e0147465.
  88. Rapp AE, Kroner J, Baur S, Schmid F, Walmsley A, Mottl H, Ignatius A. Analgesia via blockade of NGF/TrkA signaling does not influence fracture healing in mice. *J Orthop Res.* 2015;33:1235-1241.
  89. Röntgen V, Blakytyn R, Matthys R, Landauer M, Wehner T, Göckelmann M, Jermendy P, Amling M, Schinke T, Claes L, Ignatius A. Fracture healing in mice under controlled rigid and flexible conditions using an adjustable external fixator. *J Orthop Res.* 2010;28:1456-1462.
  90. Bouxsein ML, Boyd SK, Christiansen BA, Guldberg RE, Jepsen KJ, Müller R.

- 
- Guidelines for assessment of bone microstructure in rodents using micro-computed tomography. *J Bone Miner Res.* 2010;25:1468-1486.
91. Chang J, Wang Z, Tang E, Fan Z, McCauley L, Franceschi R, Guan K, Krebsbach PH, Wang CY. Inhibition of osteoblastic bone formation by nuclear factor-kappaB. *Nat Med.* 2009;15:682-689.
  92. Xian L, Wu X, Pang L, Lou M, Rosen CJ, Qiu T, Crane J, Frassica F, Zhang L, Rodriguez JP, Xiaofeng Jia, Shoshana Yakar, Shouhong Xuan, Argiris Efstratiadis, Mei Wan, Xu Cao. Matrix IGF-1 maintains bone mass by activation of mTOR in mesenchymal stem cells. *Nat Med.* 2012;18:1095-1101.
  93. Dempster DW, Compston JE, Drezner MK, Glorieux FH, Kanis JA, Malluche H, Meunier PJ, Ott SM, Recker RR, Parfitt AM. Standardized nomenclature, symbols, and units for bone histomorphometry: a 2012 update of the report of the ASBMR Histomorphometry Nomenclature Committee. *J Bone Miner Res.* 2013;28:2-17.
  94. Ehrnthaller C, Huber-Lang M, Nilsson P, Bindl R, Redeker S, Recknagel S, Rapp A, Mollnes T, Amling M, Gebhard F, Ignatius A. Complement C3 and C5 deficiency affects fracture healing. *PLoS One.* 2013;8:e81341.
  95. Kovtun A, Bergdolt S, Hägele Y, Matthes R, Lambris JD, Huber-Lang M, Ignatius A. Complement receptors C5aR1 and C5aR2 act differentially during the early immune response after bone fracture but are similarly involved in bone repair. *Sci Rep.* 2017;7:14061.
  96. Mohan S, Hu Y, Edderkaoui B. Identification of gender - specific candidate genes that influence bone microarchitecture in chromosome 1. *Calcif Tissue Int.* 2013;92:362-371.
  97. Bruick RK, McKnight SL. A conserved family of prolyl - 4 - hydroxylases that modify HIF. *Science.* 2001;294:1337-1340.
  98. Cheng S, Xing W, Pourteymoor S, Mohan S. Conditional disruption of the prolyl hydroxylase domain-containing protein 2 (Phd2) gene defines its key role in skeletal development. *J Bone Miner Res.* 2014;29:2276-2286.
  99. Bhole D, Stahl GL. Molecular basis for complement component 6 (C6)

- 
- deficiency in rats and mice. *Immunobiology*. 2004;209:559-568.
- 100.Oikonomopoulou K, Ricklin D, Ward PA, Lambris JD. Interactions between coagulation and complement--their role in inflammation. *Semin Immunopathol*. 2012;34:151-165.
  - 101.Aronovich A, Nur Y, Shezen E, Rosen C, Zlotnikov Klionsky Y, Milman I, Yarimi L, Hagin D, Rechavi G, Martinowitz U, Nagasawa T, Frenette PS, Tchorsh-Yutsis D, Reisner Y. A novel role for factor VIII and thrombin/PAR1 in regulating hematopoiesis and its interplay with the bone structure. *Blood*. 2013;122:2562-2571.
  - 102.Cole HA, Ohba T, Nyman JS, Hirotaka H, Cates JM, Flick MJ, Degen JL, Schoenecker JG. Fibrin accumulation secondary to loss of plasmin-mediated fibrinolysis drives inflammatory osteoporosis in mice. *Arthritis Rheum*. 2014;66:2222-2233.
  - 103.Turnberg D, Botto M, Warren J, Morgan BP, Walport MJ, Cook HT. CD59a deficiency exacerbates accelerated nephrotoxic nephritis in mice. *J Am Soc Nephrol*. 2003;14:2271-2279.
  - 104.Mead RJ, Neal JW, Griffiths MR, Linington C, Botto M, Lassmann H, Morgan BP. Deficiency of the complement regulator CD59a enhances disease severity, demyelination and axonal injury in murine acute experimental allergic encephalomyelitis. *Lab Invest*. 2004;84:21-28.
  - 105.Yamada K, Miwa T, Liu J, Nangaku M, Song WC. Critical protection from renal ischemia reperfusion injury by CD55 and CD59. *J Immunol* 2004;172:3869-3875.
  - 106.Weitzmann MN, Ofotokun I. Physiological and pathophysiological bone turnover-role of the immune system. *Nat Rev Endocrinol*. 2016;12:518-532.
  - 107.Cenci S, Weitzmann MN, Roggia C, Namba N, Novack D, Woodring J, Pacifici R. Estrogen deficiency induces bone loss by enhancing T-cell production of TNF-alpha. *J Clin Invest*. 2000;106:1229-1237.
  - 108.Li Y, Toraldo G, Li A, Yang X, Zhang H, Qian WP, Weitzmann MN. B cells and T cells are critical for the preservation of bone homeostasis and attainment of peak

- bone mass in vivo. *Blood*. 2007;109:3839-3848.
109. Glatt V, Canalis E, Stadmeier L, Bouxsein ML. Age-related changes in trabecular architecture differ in female and male C57BL/6J mice. *J Bone Miner Res*. 2007;22:1197-1207.
110. Halloran BP, Ferguson VL, Simske SJ, Burghardt A, Venton LL, Majumdar S. Changes in bone structure and mass with advancing age in the male C57BL/6J mouse. *J Bone Miner Res*. 2002;17:1044-1050.
111. Ferguson VL, Ayers RA, Bateman TA, Simske SJ. Bone development and age-related bone loss in male C57BL/6J mice. *Bone*. 2003;33:387-398.
112. Beamer WG, Donahue LR, Rosen CJ, Baylink DJ. Genetic variability in adult bone density among inbred strains of mice. *Bone*. 1996;18:397-403.
113. Norrdin RW, Simske SJ, Gaarde S, Schwardt JD, Thrall MA. Bone changes in mucopolysaccharidosis VI in cats and the effects of bone marrow transplantation: mechanical testing of long bones. *Bone*. 1995;17:485-489.
114. Overton TR, Basu TK. Longitudinal changes in radial bone density in older men. *Eur J Clin Nutr*. 1999;53:211-215.
115. Riggs BL, Melton LJ 3rd, O'Fallon WM. Drug therapy for vertebral fractures in osteoporosis: evidence that decreases in bone turnover and increases in bone mass both determine antifracture efficacy. *Bone*. 1996;18:197S-201S.
116. Yu W, Qin M, Xu L, van Kuijk C, Meng X, Xing X, Cao J, Genant HK. Normal changes in spinal bone mineral density in a Chinese population. *Osteoporos Int*. 1999;9:179-187.

---

## 7. List of figures and tables

- Figure 1:** Bone homeostasis is controlled by the interplay of osteoblasts, osteoclasts and osteocytes.
- Figure 2:** Osteocytes are terminally differentiated osteoblasts embedded into the bone matrix.
- Figure 3:** Role of the RANK-RANKL-OPG system in osteoclast formation.
- Figure 4:** Overview of the complement cascade with its different activation pathways.
- Figure 5:** Selected region of interest (ROI) of distal femur by  $\mu$ CT.
- Figure 6:** Selected region of interest (ROI) of lumbar spine by  $\mu$ CT.
- Figure 7:** Low bone mass and bone mineral density (BMD) of trabecular bone in femur (ROI) from 17-week-old C6-deficient (KO) mice.
- Figure 8:** Decreased bone mass of trabecular bone in spine (round ROI) from C6-deficient (KO) mice.
- Figure 9:** Increased osteoclast number and surface of trabecular bone from C6-deficient (KO) mice.
- Figure 10:** Unchanged osteoblast number and surface on trabecular bone from C6-deficient (KO) mice.
- Figure 11:** Low BMD and bone mass of trabecular bone (ROI) in femur from 17-week-old CD59a-knockout (KO) mice.
- Figure 12:** Unchanged bone mass of spine trabecular bone (round ROI) in CD59a-KO mice.
- Figure 13:** Decreased osteoclasts number of trabecular bone from CD59a-KO mice.
- Figure 14:** Unchanged osteoblast number and surface of trabecular bone from CD59a-knockout (KO) mice.
- Figure 15:** Low cortical tissue mineral density (TMD) of femur in 34-week-old C6-deficient (C6-KO) mice.
- Figure 16:** Unchanged bending stiffness of femur from C6-deficient (KO) mice.

**Figure 17:** Low cortical tissue mineral density (TMD) of femur from 17-week-old and 34-week-old CD59a-KO mice.

**Figure 18:** Increased bending stiffness (EI) and moment of inertia in X axis (MOI) of femur from 34-week-old CD59a-KO mice.

**Table 1:** Matrix proteins and their skeletal functions

**Table 2:** C6-deficient (C6-KO) mice and CD59a-knockout (CD59a-KO) mice were used for this study of skeletal phenotyping. Age- and sex-matched C57BL/6 mice were used as wild-type (WT) controls.



### **8. Acknowledgements**

First of all, I would like to express my sincere gratitude and special thanks to my supervisor Prof. Dr. Anita Ignatius, the director of Institute of Orthopaedic Research and Biomechanics at the University Hospital of Ulm, for supporting my scientific career and helping me to improve my scientific ideas and writing. I have benefited a lot from her experience, expertise, and patience.

Secondly, I also express my appreciation and gratitude to Dr. Anna Rapp, who supervised me during the process of the project, taught me more experimental skills, and helped me correct the thesis during the writing phase of dissertation. Many thanks to Yvonne Mödinger, for helping me revise the thesis so many times.

Thirdly, I would like to express my appreciation to Prof. Dr. Qin Fu, the director of Orthopaedic Department at Shengjing Hospital of China Medical University, and Prof. Dr. Bo Wu, the president of Shenyang Orthopaedic Hospital. Without their financial support, the study time in Germany would not be so productive.

In addition, many thanks to Prof. Dr. Lutz Dürselen, Prof. Dr. Hans-Joachim Wilke, Alexandra Naylor, and Werner Ohmayer, who gave me warm welcome and helped me a lot in my usual and work time.

I also want to acknowledge my colleagues, Dr. Anna Kovtun, Dr. Melanie Haffner-Luntzer, Dr. Peng Liu, and Yvonne Mödinger, who helped me a lot when I performed the histomorphometry and  $\mu$ CT experiments, thereby enriching our knowledge in this project. I also wish to give my thanks to Ursula Maile, Patrizia Horny, Iris Baum, Stefanie Schroth, and Marion Tomo, for their kind help in the technical assistance during the process of animal model, biomechanics, histomorphometry and  $\mu$ CT experiments.

Last but not least, I would like to appreciate my family and all my friends, Dr. Peng Liu, Benedikt Schlager, Kathrin Kaiser, Steffen Hacker, René Jonas, Daniela Blomberger, Margarita Darminow, Xiangxu Chen, Zhigang Meng, and Bingsheng Qin, for their support and encouragement during my research in Ulm. Without their help, I am not able to have the chance to complete this dissertation. I was enjoying my

## Acknowledgements

---

wonderful period in the Institute of Orthopaedic Research and Biomechanics at the University Hospital of Ulm, not only for the research skills but also for the life and scientific ideas. Thank you so much!

## 9. Curriculum vitae

### Personal Information

**Name:** Zhaozhou Ren

**Gender:** Male

**Year of Birth:** 1987

**Place of Birth:** Shenyang, Liaoning Province

**Nationality:** People's Republic of China

### Education

**1993-1999:** Colliery Primary School of Xima, Liaoning province, China.

**1999-2002:** Secondary Junior Middle School of Dengta, Liaoning province, China.

**2002-2005:** Senior Middle School of Dengta, Liaoning province, China.

**2005-2010:** Bachelor of Clinical Medicine, China Medical University, Shenyang, Liaoning province, China.

**2010-2013:** Master of Clinical Medicine (Surgery, Orthopaedics), Graduate School of China Medical University, Shenyang, Liaoning province, China.

**2015-now:** Doctoral student in the Faculty of Medicine, Ulm University, Germany.

### Our Publication

Mödinger Y, Rapp AE, Vikman A, Ren Z, Fischer V, Bergdolt S, Haffner-Luntzer M, Song WC, Lambris JD, Huber-Lang M, Neidlinger-Wilke C, Brenner R, Ignatius A. Reduced Terminal Complement Complex Formation in Mice Manifests in Low Bone Mass and Impaired Fracture Healing. *Am J Pathol.* 2018 Oct 17. pii: S0002-9440(18)30398-5. doi: 10.1016/j.ajpath.2018.09.011. [Epub ahead of print]